Title Page

Exosomes derived from Epstein-Barr virus-infected cells are internalized *via* caveolae-dependent endocytosis and promote phenotypic modulation in the target cells

Asuka Nanbo[a]*, Eri Kawanishi[a], Ryuji Yoshida[a], and Hironori Yoshiyama[b]

Graduate School of Pharmaceutical Sciences, Hokkaido University, N12 W6, Kita-ku, 060-0812 Sapporo, Japan[a], and Institute for Genetic Medicine, Hokkaido University, N15 W7, Kita-ku, 060-8638 Sapporo, Japan[b]

Running title; The role of exosomes derived from EBV-infected cells

*Corresponding author:

Mailing address: Graduate School of Pharmaceutical Sciences, Hokkaido University, N12 W6, Kita-ku, 060-0812 Sapporo, Japan.

Phone: +81(11)706-3244

Fax: +81(11)706-4990

Email: nanboa@pharm.hokudai.ac.jp

A.N. and E.K. contributed equally to this manuscript.

The word count for the abstract: **246**

The word count for the text: **5273**

Abstract

Epstein–Barr virus (EBV), a human gamma herpesvirus, establishes a life-long latent infection in B lymphocytes and epithelial cells following primary infection. Several lines of evidence suggest that exosomes derived from EBV-infected cells are internalized and transfer viral factors including EBV-encoded latent membrane protein and micro RNAs to the recipient cells. However the detailed mechanism by which exosomes are internalized and their physiological impact on the recipient cells are still poorly understood. Here, we visualized the internalization of fluorescently labeled exosomes derived from EBV-uninfected and EBV-infected B cells of type I, and type III latency into EBV-negative epithelial cells. In this way, we demonstrated that exosomes derived from all three cell types were internalized into the target cells in a similar fashion. Internalization of exosomes was significantly suppressed by treatment with an inhibitor of dynamin and also by the knockdown of caveolin-1. Labeled exosomes were co-localized with caveolae, and subsequently trafficked through endocytic pathways. Moreover, we observed that exosomes derived from type III latency cells up-regulated proliferation and expression of intercellular adhesion molecule 1 (ICAM-1) in the recipient cells more significantly than did those derived from EBV-negative and type I latency cells. We also identified the EBV-encoded latent membrane protein 1 (LMP1) as a gene

responsible for induction of ICAM-1 expression. Taken together, our data indicate that exosomes released from EBV-infected B cells are internalized *via* caveolae-dependent endocytosis, which in turn contribute to phenotypic changes in the recipient cells through transferring one or more viral factors.

Introduction

Epstein–Barr virus (EBV), a human gamma herpesviruses, establishes a persistent, latent infection in B lymphocytes and epithelial cells following primary infection (1). EBV has been implicated as a cause of lymphomas and epithelial malignancies such as Burkitt's lymphoma (BL), Hodgkin's disease (HD), nasopharyngeal carcinoma (NPC), and gastric carcinoma (GC).

The particular expression pattern of different latent genes defines three latency types specific to individual EBV-associated tumors [Kieff, 2001 #31] (1). EBV-encoded nuclear antigen 1 (EBNA1) is indispensable for the replication and persistence of the viral episomes in the nucleus and is consistently expressed in all types of latencies. Latency type I is associated with BL and GC, and is restricted to the expression of EBNA1, the EBV-encoded small RNAs (EBERs), and BamHI A rightward transcripts (BARTs). Latency type II, which is associated with HD and NPC, expresses EBNA1, both EBERs, BARTs, and the latent membrane proteins (LMP1, LMP2A and LMP2B). Latency type III, which is characteristic of EBV-transformed lymphoblastoid cell lines (LCLs) and post-transplant lymphoproliferative disease, expresses both the transcripts and all the EBV latent proteins, including the 6 nuclear antigens (EBNA1, EBNA2, EBNA3A, EBNA3B, EBNA3C and EBNA-LP), and three membrane proteins (LMP1, LMP2A and LMP2B).

Several lines of evidence demonstrate that EBV-infected cells secrete exosomes (2-9). Exosomes are microvesicles with diameters of 80 to 160 nm and are actively secreted into all body fluids, including blood, urine, saliva, and breast milk from various cell types (10). Exosomes are generated from the luminal membranes of multivesicular bodies (MVBs), which as late endosomes bud off parts of their membrane into their lumen to form intraluminal vesicles, and are extracellularly secreted by fusion of endosomes with the plasma membrane (11, 12). Exosomes play important roles in adaptive immune responses to pathogens and tumors by transferring proteins, soluble factors, mRNA, and microRNAs (miRNA) to the recipient cells. Previous reports demonstrated that exosomes possess a variety of functions in adaptive immune responses to pathogens and tumors by transferring specific molecules (6, 7, 13, 14). Although it has been proposed that exosomes are released from EBV-positive NPC and LCLs, their function in the recipient cells is varied and only now being elucidated. Exosomes derived from LCLs possess EBV-encoded glycoprotein gp350, which antagonizes the infection of EBV in B cells by blocking the interaction of gp350 on virions and EBV's receptor, CD21 (8). Exosomes derived from LCLs transfer viral miRNA and suppress the expression of target genes in recipient dendritic cells (DC) (5). Other reports suggest roles for EBV-encoded latent membrane protein 1 (LMP1) as an immune modulator and signaling activator, which is transferred to the target cells

via LCLs and NPC-derived exosomes. LMP1-positive exosomes derived from LCLs inhibit the proliferation of peripheral blood mononuclear cells (15). NPC cells release human leukocyte antigen (HLA) class II-positive exosomes containing LMP1 and galectin 9, which exhibit intrinsic T cell inhibitory activity (2). However, the molecular mechanism by which exosomes derived from EBV-infected cells are internalized, and the possible roles of exosomes in the phenotypic modulation of the recipient cells are not fully understood.

In the present study, we analyzed the internalization of fluorescently labeled exosomes derived from EBV-uninfected, type I, and type III latency EBV-infected cells into EBV-negative epithelial cells. In using this approach, we first showed that exosomes released from all three cell types were internalized into the target cells *via* caveolae-dependent endocytosis. We also observed that exosomes derived from type III latency cells up-regulated cell proliferation and the expression of intercellular adhesion molecule 1 (ICAM-1) in the recipient cells more than did those from EBV-negative and type I latency cells. Finally we identified EBV-encoded LMP1 as playing a role in mediating up-regulation of ICAM-1. The possible roles of exosomes derived from EBV-latently infected B cells in EBV-associated malignancies are discussed.

Materials and Methods

Cell culture

Cell lines used in this study were kindly provided by Dr. Kenzo Takada (EVEC, Inc.). Mutu I and Mutu III, which are type I and type III latency EBV-infected B cell lines, respectively, were established from the same BL tumor (16). EBV-negative subclone (Mutu$^-$) was isolated from Mutu I by the limiting dilution methods (17). LCLs were generated by transformation of the B lymphocyte component within the peripheral blood lymphocyte population by Akata EBV strain (18). Mutu$^-$, Mutu I, Mutu III, and LCLs were maintained in RPMI-1640 medium containing 10% fetal bovine serum (FBS) and antibiotics. EBV-negative human NPC cell lines, CNE1 (19-23) and HONE1 (24), a human GC cell line, NU-GC-3 (25-28), and a human lung adenocarcinoma, A549 cells (29) were grown in high-glucose Dulbecco's modified Eagle's medium (DMEM) containing 10% FBS and antibiotics. Cells were maintained at 37°C in 5% CO_2.

Purification and fluorescent labeling of exosomes

For the purification of exosomes, Mutu$^-$, Mutu I, Mutu III, or LCLs (2 x 10^8 cells, each) were grown in RPMI 1640 medium containing 10% exosome-depleted FBS, which was prepared by centrifugation at 25,000 rpm for 4 h at 4°C (30). Culture medium containing exosomes was harvested and centrifuged at 1,500 rpm for 10 min and at 6,000 rpm for 20 min to remove cells

and cell debris, respectively. The exosomes were pelleted by centrifugation at 25,000 rpm for 1 h at 4°C with an SW28 rotor (Beckman, Fullerton, USA). The pelleted exosomes were resuspended in TNE buffer [10 mM Tris-HCl (pH 7.6), 100 mM NaCl, 1 mM EDTA] over night, and fractionated by use of a 0.25-2.5 M sucrose gradient in TNE buffer at 25,000 rpm for 15 h at 4°C with an SW40 rotor (Beckman). The fractionated exosomes were pelleted at 35,000 rpm for 1 h at 4°C and resuspended in TNE buffer. The fractions containing exosomes were confirmed by western blot analysis with anti-CD63 monoclonal antibody (clone MEM-250, 1:1,000 dilution, Abnova, Taipei, Taiwan) and anti-LMP1 monoclonal antibody (clone S12, 1:10,000 dilution, kindly provided by Dr. Teruhito Yasui, Osaka University). The total protein concentration in the fractions containing exosomes was determined by the Bradford protein assay (Bio-Rad Laboratories, Hercules, USA). Exosomes were fluorescently labeled as described previously (31, 32). Briefly, 1 ml of fractionated exosomes (100 ng/ml) was incubated with 6 μl of 100 μM stock solution of 1,1'-Dioctadecyl-3,3,3',3'-Tetramethylindocarbocyanine Perchlorate (DiI) (Life technologies Carlsbad, USA) for 1 h in the dark at room temperature with gentle agitation.

Retroviral infection

Recombinant retroviruses for the expression of clathrin light chain a (CLCa)-eGFP, caveolin-1 (Cav1)-eGFP, eGFP-Rab5, eGFP-Rab7, and eGFP-CD63 were produced and purified as previously described (27, 32). For retroviral infections, CNE1, HONE1, NU-GC-3, or A549 cells grown to 20-30% confluence were incubated with viral stocks (10^7-10^8 infectious units/ml) for 1 h at 4°C at a multiplicity of infection (m.o.i) of 5. After being washed twice with complete medium, the cells were cultured in complete medium for 48 h and the expression of individual proteins were confirmed by a confocal laser scanning microscope.

Imaging of internalization of DiI-labeled exosomes in live cells

CNE1, HONE1, NU-GC-3, A549 cells, or these derivatives expressing CLCa-eGFP, Cav1-eGFP, eGFP-Rab5, eGFP-Rab7, or eGFP-CD63 were grown in 35 mm glass-bottom culture dishes (Matsunami, Osaka, Japan). DiI-exosomes derived from Mutu$^-$, Mutu I, Mutu III, or LCLs (1.5 μg, each) were adsorbed onto the cells in 50 μL of phenol red-free MEM (Life Technologies) containing 10% FBS for 30 min at room temperature. After removal of unbound exosomes by washing in the same medium, the cells were subsequently incubated for various times at 37°C. Internalization of DiI-exosomes and co-localization of DiI-exosomes with

eGFP-positive vesicles were analyzed by a confocal laser scanning microscope (Fluoview FV10i, Olympus, Osaka, Japan). Images were collected with a 60 x water objective lens (NA=1.3) (Olympus) and acquired by using FV10-ASW software (Olympus). For analysis of the internalization of exosomes, the number of DiI-exosomes was measured in 30 individual cells (approximately 5-10 dots/cell). For analysis of co-localization, the number of DiI-exosomes that co-localized with eGFP-Rab5 or eGFP-Rab7 was measured in 30 individual cells, and the percentage of co-localization in the total DiI-exosomes was determined. Co-localization percentages (proportion of co-localized DiI-exosomes with eGFP-fusion proteins to total DiI-exosomes) of individual images were analyzed by measuring the co-localization coefficient with Image J software. For the inhibitor treatment, CNE1 cells grown in 35 mm glass-bottom culture dishes were pretreated with dimethylsulfoxide (DMSO), 150 nM dynasore (Sigma-Aldrich), 75 μM 5-(N-Ethyl-N-isopropyl)amiloride (EIPA) (Sigma-Aldrich), or 20 mM NH_4Cl for 30 min at 37°C, and then incubated with DiI-exosomes for 2 h as described above in the presence of inhibitors. To analyze the inhibitory effects of dynasore or EIPA, the cells were incubated with exosomes in the presence of 1 μg/ml Alexa Fluor 647-labaled transferrin (Life technologies) for 5 min or 0.25 mg/ml Alexa Fluor 647-labeled dextran Mw 10K (Life technologies) for 2 h, respectively. Uninternalized surface-bound exosomes and Alexa Fluor

647-labeled ligands were removed by treatment with 0.25% trypsin for 1 min at 37°C and the number of intracellular DiI signals in 30 individual cells were subsequently measured by a confocal laser scanning microscope.

Cell proliferation assay

CNE1 cells (1.8 x 10^3/well) were grown in 96-well plate in DMEM containing 4% FBS in the absence or presence of 0.25 μg/mL exosomes derived from Mutu$^-$, Mutu I, or Mutu III for four days. The growth rate of the cells was measured each day with a Cell Counting Kit-8 (Dojindo, Kumamoto, Japan).

siRNA treatment and transfection

Target sequences corresponding to the human clathrin heavy chain (CHC) (33), Cav1 (34), sorting nexin 1 (SNX1) (35), and LMP1 (36)-coding sequences were selected and synthesized (Life technologies). CHC siRNA, or Cav1 and SNX1 siRNAs were transfected into CNE1, HONE1, NU-GC-3, or A549 cells by using MultiFactam (Promega, Fitchburg, USA), or TransIT-TKO (Takara Bio, Shiga, Japan), respectively. For analysis of efficiency of

down-regulation of target genes, the cells were harvested at 48 h post-transfection, fixed in 4% paraformaldehyde (PFA) for 10 min at room temperature, permeabilized with PBS containing 0.05% Triton X-100 for 10 min at room temperature, and blocked in PBS containing 1% bovine serum albumin (BSA) and 0.05% Triton X-100 for 20 min at room temperature. The cells were incubated with rabbit anti-CHC polyclonal antibody (1:200 dilution, Abcam, Cambridge, UK), rabbit anti-Cav1 polyclonal antibody (1:200 dilution, Abcam), or rabbit anti-SNX1 polyclonal antibody (1:200 dilution, Abcam) for 1 h at room temperature, respectively. The cells were then incubated with Alexa Fluor 488-labeled secondary antibodies (1:1,000 dilution, Life technologies) for 30 min at room temperature, and subjected to flow cytometric analysis (FACSCalibur, Becton, Dickinson and company, Franklin Lakes, USA). The effect of siRNA-treatment on the internalization of exosomes was analyzed by measuring the number of DiI-exosomes in 30 individual cells at 48 h post-transfection. Control or LMP1 siRNA was transfected into Mutu III cells by electropolation (Bio-Rad Gene Pulser II; 0.2 kV, 950 μF, Bio-Rad, Hercules, CA) and the effect of siRNA-treatment on ICAM-1 expression was analyzed at 48 h post-transfection. For analysis of the down-regulation of LMP1, Mutu III cells were fixed, permeabilized, and blocked as described above at 48 h post-transfection. LMP1 expression was analyzed by flow cytometric analysis using mouse anti-LMP1 antibody (clone

S12, 1:5,000 dilution). A LMP1 expression vector, which carries the simian virus 40 (SV40) promoter-driven LMP1 cDNA derived from Akata EBV strain, was transfected into Mutu$^-$ cells by electropolation and the LMP1 expression was analyzed as described above.

ICAM-1 expression assay

For analysis of ICAM-1 expression, CNE1 cells (2 x 10^5/well) were grown in a 24-well plate in the absence or presence of 0.25 μg/mL exosomes derived from Mutu$^-$, Mutu I, or Mutu III for 24 h. The cells were harvested in PBS containing 0.5 mM EDTA and fixed in 4% PFA. Cells were incubated with anti-ICAM-1 monoclonal antibody (clone Ab-2, 1:200 dilution, Thermo Scientific, Waltham, USA) for 1 h at room temperature, incubated with Alexa Fluor 488-labeled secondary antibody (1:1,000 dilution, Life technologies) for 30 min at room temperature, and subjected to flow cytometric analysis. For the exosome transfer assay, CNE1 cells (5 x 10^4/well) were grown in the basolateral chamber of 24-well transwell plate (Corning, Toledo, USA). Mutu$^-$, Mutu I, Mutu III, LMP1 siRNA-transfected Mutu III, or LMP1 expression vector-transfected Mutu$^-$ (1 x 10^5, each) were added to the membrane inserts with pore size of 0.4 μm and incubated for 3 days. CNE1 cells were harvested in PBS containing 0.5 mM EDTA, fixed in 4% PFA, and ICAM-1 expression was analyzed as described above. For the

inhibitor treatment of exosome secretion, DMSO or 10 μM GW4869 (Sigma-Aldrich) was added to the co-culture and incubated for 3 days. For the LMP1 transfer analysis, CNE1 cells (2 x 10^5/well) were grown on cover slips in the basolateral chamber of membrane inserts with a pore size of 0.4 μm. Mutu$^-$, Mutu I, or Mutu III cells (1 x 10^5, each) were added to the membrane inserts and incubated for 3 days. CNE1 cells were harvested, fixed, permeabilized, and blocked as describe above. The LMP1 localization in CNE1 cells was analyzed by immunofluorescence staining with anti-LMP1 antibody (clone S12, 1:5,000 dilution).

Results

Internalization of fluorescently labeled Mutu cells-derived exosomes in CNE1 cells.

To assess the mechanism of internalization of EBV-negative and -positive B cell-derived exosomes, we established a real-time monitoring system for fluorescently labeled exosomes. Exosomes released from EBV-uninfected Mutu$^-$, EBV-infected with type I (Mutu I), or infected with type III latency (Mutu III) were purified by sucrose gradient centrifugation [exosome (-), exosome (I), or exosome (III), respectively]. The fractions containing exosomes were determined by the expression of an exosome marker, CD63 (37). Exosome (III) showed the highest level of CD63 (Fig. 1A). We also confirmed that exosome (III) expresses LMP1, but

exosome (-) and exosome (I) were LMP1-negative (Fig. 1A). Purified exosomes were fluorescently labeled with a lipophilic tracer, DiI. We synchronized the internalization of DiI-labeled exosomes into CNE1 cells by adsorbing them for 30 min at room temperature. We then shifted the temperature to 37°C and monitored the intracellular localization of labeled exosomes by using a confocal laser scanning microscope. DiI-labeled exosome (-), exosome (I), and exosome (III), which were visualized as red particles, were internalized into CNE1 cells in a similar fashion (Fig. 1B and 1C).

Exosomes derived from Mutu cells were internalized into CNE1 cells *via* the classical endocytic pathway.

Next, we assessed the mechanism by which exosomes are internalized into CNE1 cells by treatment with inhibitors of endocytosis. Clathrin- and caveolae-mediated endocytosis depends on dynamin 2, a large GTPase that plays an essential role in vesicle scission during endocytosis (38). Treatment with a dynamin-specific inhibitor, dynasore (39) reduced the internalization of fluorescently labeled transferrin (Tf), a specific ligand of the clathrin-mediated pathway (green; Fig. 2A, top), and also the internalization of DiI-labeled exosomes (III) (red; Fig. 2A, top and 2B). These data indicate that clathrin-, and/or caveolae-mediated endocytosis is involved in the

internalization of exosomes. We also tested the effect of EIPA [5-(N-ethyl-N-isopropyl) amiloride], an inhibitor of the Na^+/H^+ exchanger that specifically inhibits macropinocytosis (40). EIPA inhibited the uptake of fluorescently labeled Dextran Mw 10,000 (Dex Mw 10K), which is a specific ligand of macropinocytosis (green; Fig. 2A, bottom), however, did not affect the internalization of exosomes (red; Fig. 2A, bottom), indicating that the internalization of exosomes is independent of macropinocytosis. We also found that the internalization of exosomes (-) and exosomes (I) is mediated by a dynamin-dependent endocytic pathway, but not by macropinocytosis (Fig. 2B).

Exosomes derived from Mutu cells and LCLs were internalized *via* a caveolae-dependent endocytic pathway into epithelial cells.

To identify the internalization pathway of exosomes, we further examined the effect of down-regulation of clathrin-heavy chain (CHC), caveolin-1 (Cav1), and sorting nexin 1 (SNX1) expression with small interfering RNAs (siRNA). CHC, Cav1, and SNX1 play roles in clathrin-, caveolae-, and macropinocytosis-mediated internalization, respectively (33-35). The effect of siRNAs on the expression of individual proteins in CNE1 cells was confirmed by flow cytometry (Fig. 3C). Down-regulation of Cav1 expression significantly suppressed the internalization of

DiI-exosome (III) (Fig. 3A and 3B), indicating that caveolae-mediated endocytosis contributes to the internalization of exosomes into CNE1 cells. However, internalization of DiI-exosomes was not blocked by down-regulation of CHC and SNX1 (Fig. 3A and 3B), further supporting the conclusion that clathrin-mediated endocytosis and macropinocytosis are not critical for their internalization. The internalization of DiI-exosome (-) and -exosome (I) was also suppressed by down-regulation of Cav1, but not by that of CHC and SNX1 (Fig. 3B).

To verify our observations are general, we also analyzed the internalization of exosomes derived from LCLs [exosome (LCL)] into a variety of human epithelial cell lines such as HONE1, NU-GC-3, and A549 cells, an EBV-negative human NPC, a human gastric cancer (GC), and a human lung adenocarcinoma cell line, respectively. We observed that internalization of exosome (LCL) were suppressed by knockdown of Cav1 significantly, but not by knockdown of CHC and SNX1 (Fig. 4). We also confirmed that exosomes (III) were internalized in these three epithelial cells *via* caveolae-dependent endocytosis (data now shown). Thus our findings demonstrate that caveolae-dependent endocytosis is a general means for internalization of exosomes derived from EBV-infected B cells into human epithelial cells.

The significance of caveolae-mediated endocytosis for the internalization of exosomes was further examined by live cell imaging. Cav1 fused to enhanced green fluorescent protein

(Cav1-eGFP), which allows visualization of individual caveolae, was expressed in CNE1, HONE1, NU-GC-3, and A549 cells. We found that DiI-exosome (III) co-localized with Cav1-eGFP in CNE1 cells (Fig. 5A, left) at 15 min after a temperature shift. On the other hand, we did not detect co-localization of eGFP-fused clathrin light chain a (CLCa-eGFP), which enabled the visualization of clathrin-coated pits, with DiI-exosomes in CNE1 cells (Fig. 5A, right). We also observed that DiI-exosomes (LCL) were efficiently co-localized with Cav1-eGFP (Fig. 5B-D, left), but not with CLC-eGFP in HONE1, NU-GC-3, and A549 cells (Fig. 5B-D, right). These results taken together show that caveolae-mediated endocytosis but not clathrin-mediated endocytosis is critical for the internalization of exosomes derived from EBV-infected cells into epithelial cells.

Internalized Mutu cell-derived exosomes trafficked to endosomal compartments.

It has been proposed that intracellular vesicles generated by caveolae-dependent endocytosis subsequently mature in endocytic vesicles (41). Here, we sought to confirm the endosomal localization of Mutu cells-derived exosomes. The small GTPases Rab5 and Rab7 specifically associate with early and late endosomes, respectively (42, 43), and serve as markers for these compartments. The tetraspanin CD63 is defined as a marker of MVB as well as late

endosomes (37). We, therefore, analyzed the co-localization of internalized DiI-labeled exosomes with eGFP-Rab5, -Rab7, or -CD63, which were stably expressed in CNE1 cells. We also assessed the kinetics of the co-localization of DiI-exosome with Rab5-, or Rab7-positive vesicles. DiI-labeled exosomes (-), (I), and (III) co-localized with eGFP-Rab5 in a time dependent manner. Co-localization of DiI-exosomes with eGFP-Rab5 reached levels of 40-60% at 40 min post-temperature shift and then decreased (Fig. 6A, left and 6B). DiI-exosomes were also co-localized with eGFP-Rab7 time-dependently with approximately 80% of DiI-exosomes co-localizing with eGFP-Rab7 within 150 min of the temperature-shift (Fig. 6A, middle and 6C). DiI-exosomes co-localized with CD63-positive vesicles in a similar fashion to that of eGFP-Rab7 (Fig. 6A, right). These results indicate that internalized exosomes trafficked through the endosomal pathway. We also found that the DiI signals were enlarged and overlapped with Rab7-positive vesicles at 5 h post-temperature shift (Fig. 6D, left). Following treatment with NH_4Cl, which inhibits the acidification of endosomes, the DiI-signals localized with eGFP-Rab7 but remained as small dots (Fig. 6D, right), suggesting that enlarged DiI was derived from the fusion of membranes of exosomes and endosomes, and that NH_4Cl inhibited this process.

The effect of Mutu cell-derived exosomes on the growth of CNE1 cells.

Previous reports indicated that expression of LMP1 in EBV-negative NPC cells promotes the release of exosomes containing fibroblast growth factor 2 (FGF-2), which up-regulates cell growth in HUVEC (44). Another report indicates that EBV-negative NPC and cervical cancer cell lines that stably express LMP1 secrete exosomes bearing LMP1, which activate growth-signaling pathways such as that of extracellular signal-regulated kinase (ERK) and Akt in HUVEC (3). Therefore we examined the effect of internalized exosomes derived from Mutu cells on the growth in CNE1 cells. We incubated CNE1 cells in the presence of exosome (-), (I), or (III) for 4 days and found that exosomes all enhanced the proliferation of CNE1 cells. Strikingly exosome (III) showed a more significant effect on cell proliferation when compared with exosome (-) and exosome (I) (Fig. 7).

The effect of exosomes derived from Mutu cells on ICAM-1 expression in CNE1 cells.

We also examined the effect of exosomes derived from Mutu cells on the expression of ICAM-1 in the recipient cells. We incubated CNE1 cells with exosome (-), (I), or (III) for 24 h and assessed the expression of ICAM-1 in CNE1 cells by flow cytometry. We found that exosomes derived from Mutu cells up-regulated the expression of ICAM-1, and exosome (III) showed the most significant effect on the up-regulation of ICAM-1 expression (Fig. 8A).

ICAM-1 expression increased at 24 hours after treatment of exosomes (Fig. 8B). Most of exosomes were co-localized with Rab7-positive vesicles in 150 min (Fig. 6C), suggesting that up-regulation of ICAM-1 is induced by *de novo* synthesis after uptake of exosomes, but not transferred *via* exosomes. We also co-cultured CNE1 cells with Mutu$^-$, Mutu I, or Mutu III cells, which were separately grown in a membrane insert for 3 days and analyzed the expression of ICAM-1 in CNE1 cells. We observed the most efficient up-regulation of ICAM-1 expression in CNE1 cells when the cells were co-cultured with Mutu III (Fig. 8C). To confirm the importance of the exosome secretion from Mutu cells, the co-cultured cells were treated with GW4869, an inhibitor of sphingomyelinase that markedly reduces exosome secretion (45). GW4869 significantly inhibited ICAM-1 expression in CNE1 cells co-cultured with Mutu III (Fig. 8C), indicating that exosomes secreted from Mutu III cells were transferred to CNE1 cells and contributed to ICAM-1 expression.

LMP1 was transferred to the target cells and was responsible for up-regulation of ICAM-1 expression.

Because it has been shown that LMP1 induces the expression of cellular proteins including ICAM-1 in EBV-infected cells (46), we assessed whether LMP1 is responsible for

exosome-mediated up-regulation of ICAM-1 expression in the recipient cells. First we tested whether LMP1 transfers from type III latency infected Mutu III cells to the recipient cells through exosomes by immunofluorescent staining. CNE1 cells co-cultured with Mutu III, but not with Mutu$^-$ or Mutu I exhibited punctate LMP1 distribution in the cytoplasm (Fig. 9A). GW4869 treatment suppressed the LMP1 signal, indicating that transfer of LMP1 was mediated by exosomes.

We further analyzed the role of LMP1 on ICAM-1 up-regulation by co-culturing CNE1 cells with Mutu$^-$ cells stably express LMP1. We confirmed the LMP1 expression level in the transfected Mutu$^-$ cells was approximately 80% of that of Mutu III at 48 h post-transfection (Fig. 9B). Co-culture with Mutu$^-$ expressing LMP1 significantly accelerated ICAM-1 expression in CNE1 cells and its up-regulation was suppressed by GW4869 treatment (Fig. 9C). We also elucidated the role of LMP1 by co-culturing CNE1 cells with Mutu III cells, which were transfected with LMP1 siRNA. Co-culture with LMP1 siRNA-treated Mutu III cells decreased ICAM-1 expression (Fig. 9D). These results together indicate that LMP1 is transferred to recipient cells from EBV-infected cells through exosomes and can induce expression of ICAM-1 in those recipient cells.

Discussion

The present study provides a tractable system to examine the internalization of exosomes in the recipient cells. We used this system to demonstrate that exosomes derived from EBV-uninfected and -latently infected B cells are internalized *via* caveolae-mediated endocytosis (Fig. 3-5) and eventually traffick through an endosomal pathway (Fig. 6).

Although accumulating evidence has shown that endocytosis followed by fusion is the dominant mode for the transfer of exosomes to target cells, a detailed mechanism by which exosomes are taken up has remained controversial. It has been proposed that exosomes derived from bone marrow DC and rat pheochromocytoma cells were endocytosed into the same cell types, respectively and eventually co-localized with various endosomal markers (47-49). Exosomes-derived from B lymphocytes and cervical cancer cells were distributed in the intracellular compartment in DC and HUVEC, respectively (3, 5). One report indicates that exosomes derived from human erythroleukemia and human T-lymphotropic virus (HTLV)-transformed T cell leukemia cells are internalized into phagocytic cells *via* phagocytosis (50). Further investigation will be required to determine whether caveolae-mediated endocytosis is a general pathway for the internalization of exosomes through use of the combinations of cell types as donors and recipients. It has been proposed that an acidic

environment is important for transfer of exosomes to recipient cells (51, 52), indicating that low pH-dependent membrane fusion of exosomes is critical for transfer of exosomes. However it has not been shown whether exosomes fuse at the cell surface or with endosomal membranes. We first visualized membrane fusion of exosomes in the endosomal compartment and demonstrated that this process is low-pH-dependent (Fig. 6D), suggesting that the exosomal contents and exosome-bearing membrane proteins are subsequently released into the cytoplasm and to endosomal membranes, respectively.

The molecular basis of internalization and membrane fusion of exosomes has been under study. It has been shown that exosomes of various cellular origins preferentially target specific cell types. For example DC-derived exosomes mainly interact with monocytes but not with B cells (8). In contrast, exosomes derived from LCLs preferentially target B cells (8). Previous observations suggest that target-cell preference of exosomes is dependent on some specific combination of protein-protein interactions. Antibody-blocking studies showed that the uptake of exosomes by target cells is mediated by ligand-receptor interactions such as tetraspanin-complexes and adhesion molecules (47, 53-57). Exosomes derived from LCLs carry an EBV's glycoprotein, gp350 and then preferentially target B cells by an interaction with its ligand, CD21 (8). Because exosome (-), (I), and (III) were internalized in a similar fashion

(Fig. 1C and D), the molecules commonly expressed on exosomes derived from Mutu cells likely contribute to their attachment to target cell surfaces and their subsequent internalization. Proteomic analysis has revealed that exosomes derived from B cells possess a variety of molecules including major histocompatibility complex (MHC) molecules, heat shock proteins, and tetraspanins (58). Identification of the molecules both on exosomes and the surfaces of recipient cells involved in the uptake of exosomes should allow us to understand the molecular basis of this process.

We demonstrate that exosomes (III) when added to recipients mediated proliferation and up-regulation of ICAM-1 more robustly than did exosomes (-) and (I) (Fig. 7 and 8). We also identified EBV-encoded LMP1 is one of key factors that contributes to ICAM-1 up-regulation (Fig. 9). LMP1 is defined as a viral oncogene that contributes to EBV-induced transformation of B lymphocytes and Rat-1 fibroblasts by activation of a variety of signaling pathways (59-62). Exosomes-bearing LMP1 are released from type II (2, 15) and III (9, 15, 63) latency EBV-infected cells. NPC and cervical carcinoma cells that are stably expressing LMP1 transferred this molecule to the target cells *via* exosomes, resulting in the activation of the ERK and Akt signaling pathways (3). It has been also shown that LMP1 can induce the expression of cellular adhesion molecules including ICAM-1 in various cell types (46, 64, 65).

One hypothesis to explain these findings involves exosome (III)-mediated transfer of LMP1 which up-regulate cell growth by activation of cell signaling pathways, and also induces *de novo* ICAM-1 expression in the recipient cells. Alternatively LMP1 could up-regulates the expression of the epidermal growth factor receptor (3) and FGF-2 (44), to concentrate them in the secreted exosomes. This alternative hypothesis would mean that exosome (III) transfers growth factors and/or their receptors, which subsequently influence the phenotypes of target cells. Transferred LMP1 exhibited a cytoplasmic punctate distribution (Fig. 9A). A previous report demonstrated that LMP1 signals from intracellular compartments containing lipid rafts (66). Another report indicates that LMP1 distributes within intraluminal vesicles of MVB to escape its degradation (9). Therefore, internalized exosomes likely release LMP1 to endosomal membranes following low-pH dependent membrane fusion.

Treatment with exosome (I) and co-culture with Mutu I cells also showed a slight up-regulation of cell growth and ICAM-1 expression in the recipient cells when compared with exosome (-) treatment and co-culture with Mutu^{-} (Fig. 7 and 8), indicating that type I latency specific viral factors are also responsible for these phenotypic modulations. It has been demonstrated that EBV-encoded noncoding regulatory miRNAs are transferred to target cells through exosomes (3, 5) and subsequently down-regulate their targets gene (5). The pattern of

expression of viral miRNAs varies among EBV-latently infected cells. For example, the expression of EBV's BART miRNAs differs between Mutu I and Mutu III (67). Therefore it will be important to investigate which viral and/or cellular miRNAs are transferred to target cells *via* exosomes and how they contribute to phenotypic changes.

It has also been proposed that ICAM-1 is involved in the process of invasion and metastasis in a variety of cancers (68-71). Although elevated levels of the expression of ICAM-1 in EBV-positive NPC cells have been reported (72), their significance in NPC has not been elucidated. Previous observations demonstrate that infection of epithelial cells with EBV is predominately mediated by cell-to-cell contact (73-78). Exosomes may stabilize cell-to-cell contact between EBV-infected cells and epithelial cells by transferring adherent molecules, and facilitate EBV infection into target epithelial cells. Because it has been shown that treatment of HUVEC with chronic myelogenous leukemia cells-derived exosomes induces up-regulation of ICAM-1, expression of vascular cell adhesion molecule (VCAM)-1, and contributes to angiogenesis (14), the roles of exosomes derived from EBV-infected cells in various cell types should be further assessed. Moreover a proteomic analysis is required to identify additional target proteins induced by uptake of exosomes in recipient cells.

In this context, the inhibition of either exosome shedding or blockage of exosome functions

has been proposed as an approach to cancer therapy (79). Our findings indicate that both blocking exosome secretion from EBV-infected cells and their internalization into target cells could be useful therapeutic targets for EBV-associated tumors including NPC.

Acknowledgement

We acknowledge Drs Kenzo Takada (EVEC, Inc.) and Teruhito Yasui (Osaka University) for providing cell lines and anti-LMP1 antibody, respectively. We also thank Drs Bill Sugden (University of Wisconsin, Madison) and Yusuke Ohba (Hokkaido University) for critically reviewing the manuscript. This work was supported by grants-in-aid from the Japanese Ministry of Education, Science, Sports, Culture, and Technology, Japan.

References

1. **Kieff E, Rickinson AB.** 2001. Epstein-Barr virus and its replication. In M. Knipe and P. M. Howley (ed.), Fields virology, 4th ed. Lippincott Williams & Wilkins, Philadelphia, PA**:**2511-2573.

2. **Keryer-Bibens C, Pioche-Durieu C, Villemant C, Souquere S, Nishi N, Hirashima M, Middeldorp J, Busson P.** 2006. Exosomes released by EBV-infected nasopharyngeal carcinoma cells convey the viral latent membrane protein 1 and the immunomodulatory protein galectin 9. BMC Cancer **6:**283.

3. **Meckes DG, Jr., Shair KH, Marquitz AR, Kung CP, Edwards RH, Raab-Traub N.** 2010. Human tumor virus utilizes exosomes for intercellular communication. Proc Natl Acad Sci U S A **107:**20370-20375.

4. **Middeldorp JM, Pegtel DM.** 2008. Multiple roles of LMP1 in Epstein-Barr virus induced immune escape. Semin Cancer Biol **18:**388-396.

5. **Pegtel DM, Cosmopoulos K, Thorley-Lawson DA, van Eijndhoven MA, Hopmans ES, Lindenberg JL, de Gruijl TD, Wurdinger T, Middeldorp JM.** 2010. Functional delivery of viral miRNAs via exosomes. Proc Natl Acad Sci U S A **107:**6328-6333.

6. **Pegtel DM, van de Garde MD, Middeldorp JM.** 2011. Viral miRNAs exploiting the endosomal-exosomal pathway for intercellular cross-talk and immune evasion. Biochim Biophys Acta **1809:**715-721.

7. **Raposo G, Nijman HW, Stoorvogel W, Liejendekker R, Harding CV, Melief CJ, Geuze HJ.** 1996. B lymphocytes secrete antigen-presenting vesicles. J Exp Med **183:**1161-1172.

8. **Vallhov H, Gutzeit C, Johansson SM, Nagy N, Paul M, Li Q, Friend S, George TC, Klein E, Scheynius A, Gabrielsson S.** 2011. Exosomes containing glycoprotein 350 released by EBV-transformed B cells selectively target B cells through CD21 and block EBV infection in vitro. J Immunol **186:**73-82.

9. **Verweij FJ, van Eijndhoven MA, Hopmans ES, Vendrig T, Wurdinger T, Cahir-McFarland E, Kieff E, Geerts D, van der Kant R, Neefjes J, Middeldorp JM, Pegtel DM.** 2011. LMP1 association with CD63 in endosomes and secretion via exosomes limits constitutive NF-kappaB activation. EMBO J **30:**2115-2129.

10. **Sokolova V, Ludwig AK, Hornung S, Rotan O, Horn PA, Epple M, Giebel B.** 2011. Characterisation of exosomes derived from human cells by nanoparticle tracking analysis and scanning electron microscopy. Colloids Surf B Biointerfaces **87:**146-150.

11. **Johnstone RM, Adam M, Hammond JR, Orr L, Turbide C.** 1987. Vesicle formation during reticulocyte maturation. Association of plasma membrane activities with released vesicles (exosomes). J Biol Chem **262:**9412-9420.

12. **Wollert T, Hurley JH.** 2010. Molecular mechanism of multivesicular body biogenesis by ESCRT complexes. Nature **464:**864-869.

13. **Raposo G, Stoorvogel W.** 2013. Extracellular vesicles: Exosomes, microvesicles, and friends. J Cell Biol **200:**373-383.

14. **Taverna S, Flugy A, Saieva L, Kohn EC, Santoro A, Meraviglia S, De Leo G, Alessandro R.** 2011. Role of exosomes released by chronic myelogenous leukemia cells in angiogenesis. Int J Cancer **130:**2033-2043.

15. **Flanagan J, Middeldorp J, Sculley T.** 2003. Localization of the Epstein-Barr virus protein LMP 1 to exosomes. J Gen Virol **84:**1871-1879.

16. **Gregory CD, Rowe M, Rickinson AB.** 1990. Different Epstein-Barr virus-B cell interactions in phenotypically distinct clones of a Burkitt's lymphoma cell line. J Gen Virol **71 (Pt 7):**1481-1495.

17. **Kitagawa N, Goto M, Kurozumi K, Maruo S, Fukayama M, Naoe T, Yasukawa M, Hino K, Suzuki T, Todo S, Takada K.** 2000. Epstein-Barr virus-encoded poly(A)(-) RNA supports Burkitt's lymphoma growth through interleukin-10 induction. EMBO J

19:6742-6750.

18. **von Knebel Doeberitz M, Bornkamm GW, zur Hausen H.** 1983. Establishment of spontaneously outgrowing lymphoblastoid cell lines with Cyclosporin A. Med Microbiol Immunol **172:**87-99.

19. **Iwakiri D, Sheen TS, Chen JY, Huang DP, Takada K.** 2005. Epstein-Barr virus-encoded small RNA induces insulin-like growth factor 1 and supports growth of nasopharyngeal carcinoma-derived cell lines. Oncogene **24:**1767-1773.

20. **Seto E, Ooka T, Middeldorp J, Takada K.** 2008. Reconstitution of nasopharyngeal carcinoma-type EBV infection induces tumorigenicity. Cancer Res **68:**1030-1036.

21. **Seto E, Yang L, Middeldorp J, Sheen TS, Chen JY, Fukayama M, Eizuru Y, Ooka T, Takada K.** 2005. Epstein-Barr virus (EBV)-encoded BARF1 gene is expressed in nasopharyngeal carcinoma and EBV-associated gastric carcinoma tissues in the absence of lytic gene expression. J Med Virol **76:**82-88.

22. **Sizhong Z, Xiukung G, Yi Z.** 1983. Cytogenetic studies on an epithelial cell line derived from poorly differentiated nasopharyngeal carcinoma. Int J Cancer **31:**587-590.

23. **Zhang S, Wu Y, Zeng Y, Zech L, Klein G.** 1982. Cytogenetic studies on an epithelioid cell line derived from nasopharyngeal carcinoma. Hereditas **97:**23-28.

24. **Yao KT, Zhang HY, Zhu HC, Wang FX, Li GY, Wen DS, Li YP, Tsai CH, Glaser R.** 1990. Establishment and characterization of two epithelial tumor cell lines (HNE-1 and HONE-1) latently infected with Epstein-Barr virus and derived from nasopharyngeal carcinomas. Int J Cancer **45:**83-89.

25. **Akiyama S, Amo H, Watanabe T, Matsuyama M, Sakamoto J, Imaizumi M, Ichihashi H, Kondo T, Takagi H.** 1988. Characteristics of three human gastric cancer cell lines, NU-GC-2, NU-GC-3 and NU-GC-4. Jpn J Surg **18:**438-446.

26. **Iwakiri D, Eizuru Y, Tokunaga M, Takada K.** 2003. Autocrine growth of Epstein-Barr

virus-positive gastric carcinoma cells mediated by an Epstein-Barr virus-encoded small RNA. Cancer Res **63:**7062-7067.

27. **Kennedy G, Sugden B.** 2003. EBNA-1, a bifunctional transcriptional activator. Mol Cell Biol **23:**6901-6908.

28. **Yoshiyama H, Imai S, Shimizu N, Takada K.** 1997. Epstein-Barr virus infection of human gastric carcinoma cells: implication of the existence of a new virus receptor different from CD21. J Virol **71:**5688-5691.

29. **Giard DJ, Aaronson SA, Todaro GJ, Arnstein P, Kersey JH, Dosik H, Parks WP.** 1973. In vitro cultivation of human tumors: establishment of cell lines derived from a series of solid tumors. J Natl Cancer Inst **51:**1417-1423.

30. **Eldh M, Lotvall J, Malmhall C, Ekstrom K.** 2012. Importance of RNA isolation methods for analysis of exosomal RNA: evaluation of different methods. Mol Immunol **50:**278-286.

31. **Kawamoto T, Ohga N, Akiyama K, Hirata N, Kitahara S, Maishi N, Osawa T, Yamamoto K, Kondoh M, Shindoh M, Hida Y, Hida K.** 2012. Tumor-derived microvesicles induce proangiogenic phenotype in endothelial cells via endocytosis. PLoS One **7:**e34045.

32. **Nanbo A, Imai M, Watanabe S, Noda T, Takahashi K, Neumann G, Halfmann P, Kawaoka Y.** 2010. Ebolavirus is internalized into host cells via macropinocytosis in a viral glycoprotein-dependent manner. PLoS Pathog **6:**e1001121.

33. **Moskowitz HS, Yokoyama CT, Ryan TA.** 2005. Highly cooperative control of endocytosis by clathrin. Mol Biol Cell **16:**1769-1776.

34. **Manninen A, Verkade P, Le Lay S, Torkko J, Kasper M, Fullekrug J, Simons K.** 2005. Caveolin-1 is not essential for biosynthetic apical membrane transport. Mol Cell Biol **25:**10087-10096.

35. **Kerr MC, Lindsay MR, Luetterforst R, Hamilton N, Simpson F, Parton RG, Gleeson PA, Teasdale RD.** 2006. Visualisation of macropinosome maturation by the recruitment of sorting nexins. J Cell Sci **119:**3967-3980.

36. **Mei YP, Zhu XF, Zhou JM, Huang H, Deng R, Zeng YX.** 2006. siRNA targeting LMP1-induced apoptosis in EBV-positive lymphoma cells is associated with inhibition of telomerase activity and expression. Cancer Lett **232:**189-198.

37. **Escola JM, Kleijmeer MJ, Stoorvogel W, Griffith JM, Yoshie O, Geuze HJ.** 1998. Selective enrichment of tetraspan proteins on the internal vesicles of multivesicular endosomes and on exosomes secreted by human B-lymphocytes. J Biol Chem **273:**20121-20127.

38. **Orth JD, Krueger EW, Cao H, McNiven MA.** 2002. The large GTPase dynamin regulates actin comet formation and movement in living cells. Proc Natl Acad Sci U S A **99:**167-172.

39. **Newton AJ, Kirchhausen T, Murthy VN.** 2006. Inhibition of dynamin completely blocks compensatory synaptic vesicle endocytosis. Proc Natl Acad Sci U S A **103:**17955-17960.

40. **Koivusalo M, Welch C, Hayashi H, Scott CC, Kim M, Alexander T, Touret N, Hahn KM, Grinstein S.** 2010. Amiloride inhibits macropinocytosis by lowering submembranous pH and preventing Rac1 and Cdc42 signaling. J Cell Biol **188:**547-563.

41. **Engel S, Heger T, Mancini R, Herzog F, Kartenbeck J, Hayer A, Helenius A.** 2011. Role of endosomes in simian virus 40 entry and infection. J Virol **85:**4198-4211.

42. **Chavrier P, Parton RG, Hauri HP, Simons K, Zerial M.** 1990. Localization of low molecular weight GTP binding proteins to exocytic and endocytic compartments. Cell **62:**317-329.

43. **Rybin V, Ullrich O, Rubino M, Alexandrov K, Simon I, Seabra MC, Goody R, Zerial M.** 1996. GTPase activity of Rab5 acts as a timer for endocytic membrane fusion. Nature **383:**266-269.

44. **Ceccarelli S, Visco V, Raffa S, Wakisaka N, Pagano JS, Torrisi MR.** 2007. Epstein-Barr virus latent membrane protein 1 promotes concentration in multivesicular bodies of fibroblast growth factor 2 and its release through exosomes. Int J Cancer **121:**1494-1506.

45. **Trajkovic K, Hsu C, Chiantia S, Rajendran L, Wenzel D, Wieland F, Schwille P, Brugger B, Simons M.** 2008. Ceramide triggers budding of exosome vesicles into multivesicular endosomes. Science **319:**1244-1247.

46. **Wang F, Gregory C, Sample C, Rowe M, Liebowitz D, Murray R, Rickinson A, Kieff E.** 1990. Epstein-Barr virus latent membrane protein (LMP1) and nuclear proteins 2 and 3C are effectors of phenotypic changes in B lymphocytes: EBNA-2 and LMP1 cooperatively induce CD23. J Virol **64:**2309-2318.

47. **Morelli AE, Larregina AT, Shufesky WJ, Sullivan ML, Stolz DB, Papworth GD, Zahorchak AF, Logar AJ, Wang Z, Watkins SC, Falo LD, Jr., Thomson AW.** 2004. Endocytosis, intracellular sorting, and processing of exosomes by dendritic cells. Blood **104:**3257-3266.

48. **Tian T, Wang Y, Wang H, Zhu Z, Xiao Z.** 2010. Visualizing of the cellular uptake and intracellular trafficking of exosomes by live-cell microscopy. J Cell Biochem **111:**488-496.

49. **Tian T, Zhu YL, Hu FH, Wang YY, Huang NP, Xiao ZD.** 2012. Dynamics of exosome internalization and trafficking. J Cell Physiol.

50. **Feng D, Zhao WL, Ye YY, Bai XC, Liu RQ, Chang LF, Zhou Q, Sui SF.** 2010. Cellular internalization of exosomes occurs through phagocytosis. Traffic **11:**675-687.

51. **Taraboletti G, D'Ascenzo S, Giusti I, Marchetti D, Borsotti P, Millimaggi D, Giavazzi R, Pavan A, Dolo V.** 2006. Bioavailability of VEGF in tumor-shed vesicles depends on vesicle burst induced by acidic pH. Neoplasia **8:**96-103.

52. **Parolini I, Federici C, Raggi C, Lugini L, Palleschi S, De Milito A, Coscia C, Iessi E, Logozzi M, Molinari A, Colone M, Tatti M, Sargiacomo M, Fais S.** 2009. Microenvironmental pH is a key factor for exosome traffic in tumor cells. J Biol Chem **284:**34211-34222.

53. **Koumangoye RB, Sakwe AM, Goodwin JS, Patel T, Ochieng J.** 2011. Detachment of breast tumor cells induces rapid secretion of exosomes which subsequently mediate cellular adhesion and spreading. PLoS One **6:**e24234.

54. **Nazarenko I, Rana S, Baumann A, McAlear J, Hellwig A, Trendelenburg M, Lochnit G, Preissner KT, Zoller M.** 2010. Cell surface tetraspanin Tspan8 contributes to molecular pathways of exosome-induced endothelial cell activation. Cancer Res **70:**1668-1678.

55. **Nolte-'t Hoen EN, Buschow SI, Anderton SM, Stoorvogel W, Wauben MH.** 2009. Activated T cells recruit exosomes secreted by dendritic cells via LFA-1. Blood **113:**1977-1981.

56. **Rana S, Yue S, Stadel D, Zoller M.** 2012. Toward tailored exosomes: the exosomal tetraspanin web contributes to target cell selection. Int J Biochem Cell Biol **44:**1574-1584.

57. **Thery C, Boussac M, Veron P, Ricciardi-Castagnoli P, Raposo G, Garin J, Amigorena S.** 2001. Proteomic analysis of dendritic cell-derived exosomes: a secreted subcellular compartment distinct from apoptotic vesicles. J Immunol **166:**7309-7318.

58. **Wubbolts R, Leckie RS, Veenhuizen PT, Schwarzmann G, Mobius W, Hoernschemeyer J, Slot JW, Geuze HJ, Stoorvogel W.** 2003. Proteomic and biochemical analyses of human B cell-derived exosomes. Potential implications for their function and multivesicular body formation. J Biol Chem **278:**10963-10972.

59. **Wang D, Liebowitz D, Kieff E.** 1985. An EBV membrane protein expressed in immortalized lymphocytes transforms established rodent cells. Cell **43:**831-840.

60. **Sugden B.** 1989. An intricate route to immortality. Cell **57:**5-7.

61. **Kaye KM, Izumi KM, Kieff E.** 1993. Epstein-Barr virus latent membrane protein 1 is essential for B-lymphocyte growth transformation. Proc Natl Acad Sci U S A **90:**9150-9154.

62. **Mainou BA, Everly DN, Jr., Raab-Traub N.** 2005. Epstein-Barr virus latent membrane protein 1 CTAR1 mediates rodent and human fibroblast transformation through activation of PI3K. Oncogene **24:**6917-6924.

63. **Dukers DF, Meij P, Vervoort MB, Vos W, Scheper RJ, Meijer CJ, Bloemena E, Middeldorp JM.** 2000. Direct immunosuppressive effects of EBV-encoded latent membrane protein 1. J Immunol **165:**663-670.

64. **Mehl AM, Floettmann JE, Jones M, Brennan P, Rowe M.** 2001. Characterization of intercellular adhesion molecule-1 regulation by Epstein-Barr virus-encoded latent membrane protein-1 identifies pathways that cooperate with nuclear factor kappa B to activate transcription. J Biol Chem **276:**984-992.

65. **Peng M, Lundgren E.** 1993. Transient expression of the Epstein-Barr virus LMP1 gene in B-cell chronic lymphocytic leukemia cells, T cells, and hematopoietic cell lines: cell-type-independent-induction of CD23, CD21, and ICAM-1. Leukemia **7:**104-112.

66. **Lam N, Sugden B.** 2003. LMP1, a viral relative of the TNF receptor family, signals principally from intracellular compartments. EMBO J **22:**3027-3038.

67. **Pratt ZL, Kuzembayeva M, Sengupta S, Sugden B.** 2009. The microRNAs of Epstein-Barr Virus are expressed at dramatically differing levels among cell lines. Virology **386:**387-397.

68. **Tempia-Caliera AA, Horvath LZ, Zimmermann A, Tihanyi TT, Korc M, Friess H, Buchler MW.** 2002. Adhesion molecules in human pancreatic cancer. J Surg Oncol **79:**93-100.

69. **Rosette C, Roth RB, Oeth P, Braun A, Kammerer S, Ekblom J, Denissenko MF.** 2005. Role of ICAM1 in invasion of human breast cancer cells. Carcinogenesis **26:**943-950.

70. **Roland CL, Harken AH, Sarr MG, Barnett CC, Jr.** 2007. ICAM-1 expression determines malignant potential of cancer. Surgery **141:**705-707.

71. **Johnson JP, Stade BG, Holzmann B, Schwable W, Riethmuller G.** 1989. De novo expression of intercellular-adhesion molecule 1 in melanoma correlates with increased risk of metastasis. Proc Natl Acad Sci U S A **86:**641-644.

72. **Busson P, Zhang Q, Guillon JM, Gregory CD, Young LS, Clausse B, Lipinski M, Rickinson AB, Tursz T.** 1992. Elevated expression of ICAM1 (CD54) and minimal expression of LFA3 (CD58) in Epstein-Barr-virus-positive nasopharyngeal carcinoma cells. Int J Cancer **50:**863-867.

73. **Tao Q, Srivastava G, Chan AC, Ho FC.** 1995. Epstein-Barr-virus-infected nasopharyngeal intraepithelial lymphocytes. Lancet **345:**1309-1310.

74. **Speck P, Longnecker R.** 2000. Infection of breast epithelial cells with Epstein-Barr virus via cell-to-cell contact. J Natl Cancer Inst **92:**1849-1851.

75. **Shannon-Lowe CD, Neuhierl B, Baldwin G, Rickinson AB, Delecluse HJ.** 2006. Resting B cells as a transfer vehicle for Epstein-Barr virus infection of epithelial cells. Proc Natl Acad Sci U S A **103:**7065-7070.

76. **Shannon-Lowe C, Rowe M.** 2011. Epstein-Barr virus infection of polarized epithelial cells via the basolateral surface by memory B cell-mediated transfer infection. PLoS Pathog **7:**e1001338.

77. **Nanbo A, Terada H, Kachi K, Takada K, Matsuda T.** 2012. Roles of cell signaling pathways in cell-to-cell contact-mediated Epstein-Barr virus transmission. J Virol **86:**9285-9296.

78. **Chang Y, Tung CH, Huang YT, Lu J, Chen JY, Tsai CH.** 1999. Requirement for cell-to-cell contact in Epstein-Barr virus infection of nasopharyngeal carcinoma cells and keratinocytes. J Virol **73:**8857-8866.

79. **Viaud S, Thery C, Ploix S, Tursz T, Lapierre V, Lantz O, Zitvogel L, Chaput N.** 2010. Dendritic cell-derived exosomes for cancer immunotherapy: what's next? Cancer Res **70:**1281-1285.

Figure Legends

Fig. 1. Internalization of exosomes derived from Mutu cells into EBV-negative NPC cells.

(A) Purified exosomes derived from EBV-negative, latency type I, and type III EBV-infected Mutu cells. (Left) Exosomes were purified from culture medium of Mutu$^-$ (1st lane), Mutu I (2nd lane), and Mutu III (3rd lane) cells. 4 μg of exosomes were analyzed by western blot with anti-CD63 and LMP1 monoclonal antibodies. The arrow indicates the bands that correspond to CD63. (Right) Transferred proteins on the membrane were stained with Coomassie Brilliant Blue R-250. (B) Internalization of DiI-labeled exosomes derived from Mutu cells into CNE1 cells. After adsorption of DiI-labeled exosome (-) (left), exosome (I) (middle), or exosome (III) (right) at room temperature for 30 min, CNE1 cells were incubated at 37˚C for 2 h and intracellular DiI signals (red) were monitored by use of a confocal laser scanning microscope. Scale bars: 20 μm. Outlines of individual cells are drawn in white. (C) Quantitative analysis of the internalization of DiI-exosomes into CNE1 cells. At 2 h post-temperature shift, the numbers of internalized DiI-exosomes were measured in 30 individual CNE1 cells. Each experiment was performed in triplicate and the average and its standard deviation (SD) are shown in each condition.

Fig. 2. The effect of endocytosis inhibitors on the internalization of exosomes derived from Mutu cells into target cells.

(A) The effect of endocytosis inhibitors on the internalization of DiI-exosomes. CNE1 cells were pretreated with DMSO, dynasore, or EIPA for 30 min at 37°C, and then incubated with DiI-exosome (III) for 2 h at 37°C in the presence of inhibitors. To confirm the inhibitory effects of dynasore or EIPA, the same cells were treated with exosomes with Alexa Fluor 647-transferrin (AF-Tf) for 5 min, or Alexa Fluor 647-dextran Mw 10K (AF-Dex Mw 10K) for 2 h, respectively. After removal of surface-bound exosomes and ligands, internalized DiI-exosome (III) (red) and Alexa Fluor-labeled ligands (green) was analyzed by using a confocal laser scanning microscope. The nuclei were stained with Hoechst 33342 (blue). Scale bars, 20 μm. (B) Quantitative analysis of the effect of endocytosis inhibitors on the internalization of DiI-exosomes. CNE1 cells were pretreated with individual inhibitors for 30 min at 37°C, and then incubated with DiI-exosomes for 2 h at 37°C in the presence of inhibitors. At 2 h post-temperature shift, the number of internalized DiI-exosomes (-) (white), exosomes (I) (gray), or exosomes (III) (black) was measured in 30 individual cells. Each experiment was performed in triplicate and the average and its SD are shown in each condition. **, $P < 0.01$ versus respective control (Student's *t* test).

Fig. 3. The effect of siRNA treatment on the internalization of exosomes derived from Mutu cells into target cells.

(A) The effect of siRNA treatment on the internalization of DiI-exosomes. CNE1 cells were transfected with control siRNA or siRNA to down-regulate Cav1, CHC, or SNX1 expression. DiI-exosomes (III) were adsorbed on to the cells at 48 h post-transfection, and incubated for 2 h at 37°C. After removal of surface-bound DiI-exosomes, intracellular DiI signals (red) were analyzed by use of a confocal laser scanning microscope. Outlines of individual cells were drawn in white. Scale bars, 20 μm. (B) Quantitative analysis of the effect of siRNA treatment on the internalization of exosomes. The numbers of DiI-exosomes (-) (white), exosomes (I) (gray), or exosomes (III) (black) in 30 individual cells were measured. Each experiment was performed in triplicate and the results are presented as the mean ± SD. **, $P < 0.01$ versus respective control (Student's *t* test). (C) The efficiency of down-regulation of target genes by siRNA treatment. The efficiency of down-regulation of individual target proteins in CNE1 cells was analyzed by flow cytometry at 48 h post-transfection. Each experiment was performed in triplicate and the results are presented as the mean ± SD. *, $P < 0.05$ versus respective control (Student's *t* test).

Fig. 4. The effect of siRNA treatment on the internalization of exosomes derived from LCLs into a variety of EBV-negative epithelial cells.

(A) Quantitative analysis of effect of siRNA treatment on the internalization of exosomes derived from LCLs into epithelial cells. HONE1, NU-GC-3, or A549 cells were transfected with control siRNA or siRNA to down-regulate Cav1, CHC, or SNX1 expression. DiI-exosomes (LCL) were adsorbed on to the cells at 48 h post-transfection, and incubated for 2 h at 37°C. After removal of surface-bound DiI-exosomes, the number of intracellular DiI signals was analyzed in 30 individual cells by use of a confocal laser scanning microscope. Each experiment was performed in triplicate and the results are presented as the mean ± SD. *, $P < 0.05$ versus respective control (Student's *t* test). (B-D) The efficiency of down-regulation of target genes by siRNA treatment in HONE1 (B), NU-GC-3 (C), and A549 cells (D). The efficiency of down-regulation of individual target proteins was analyzed by flow cytometry at 48 h post-transfection. Each experiment was performed in triplicate and the results are presented as the mean ± SD. *, $P < 0.05$ versus respective control (Student's *t* test).

Fig. 5. DiI-labeled exosomes co-localize with Cav1-eGFP.

CNE1 (A), HONE1 (B), NU-GC-3 (C), or A549 cells (D) stably expressing Cav1-eGFP or CLCa-eGFP were grown in 35 mm glass-bottom culture dishes. DiI-exosomes (III) or DiI-exosomes (LCL) were adsorbed on to the cells and the cells were incubated for various times at 37°C after removal of unbound exosomes. Co-localization of DiI signals (red) with Cav1-eGFP (green; left) or CLCa-eGFP (green; right) was analyzed by a confocal laser scanning microscope at 15 min post-temperature shift. Insets show DiI-exosomes (red), Cav1-eGFP (green), and merged images of the boxed areas. Co-localized signals are indicated by white arrows. The percentage of co-localization (proportion of co-localized DiI-exosomes with eGFP-fusion proteins to total DiI-exosomes) is shown in the individual panel. Scale bars: 10 μm.

Fig. 6. Internalized DiI-exosomes traffick through the endosomal pathway.

(A) Co-localization of DiI-exosomes with endosomes. CNE1 cells stably expressing eGFP-Rab5, eGFP-Rab7, or eGFP-CD63 were grown in 35 mm glass-bottom culture dishes. DiI-exosomes were adsorbed to the cells and the cells were incubated for various times at 37°C

after removal of unbound exosomes. Co-localization of DiI signals (red) with eGFP-Rab5 (green; left), eGFP-Rab7 (green; middle), or eGFP-CD63 (green; right) was analyzed by a confocal laser scanning microscope at indicated time points after a temperature-shift. Insets show DiI-exosomes (red), eGFP-positive vesicles (green), and merged images of the boxed areas. White arrows indicate co-localized signals. The percentage of co-localization (proportion of co-localized DiI-exosomes with eGFP-fusion proteins to total DiI-exosomes) is shown in the individual panels. Scale bars: 20 μm. (B) Kinetics of co-localization of DiI-exosomes with eGFP-Rab5. Shown are the co-localization efficiencies of DiI-exosomes (-) (white), exosomes (I) (gray), or exosomes (III) (black) with eGFP-Rab5 at the indicated time points after a temperature shift to 37°C. The number of co-localized DiI-exosomes with eGFP-Rab5 was measured in 30 individual cells and the percentage of co-localization in the total DiI-exosomes is shown. Each experiment was performed in triplicate and the results are presented as the mean ± SD. (C) Kinetics of co-localization of DiI-exosomes with eGFP-Rab7. Shown are the co-localization efficiencies of DiI-exosomes (-) (white), exosomes (I) (gray), or exosomes (III) (black) with eGFP-Rab7 at the indicated time points after a temperature shift to 37°C. The number of co-localized DiI-exosomes with eGFP-Rab7-positive vesicles was measured in 30 individual cells and the percentage of co-localization in the total DiI-exosomes is shown. Each

experiment was performed in triplicate and the results are presented as the mean ± SD. (D) The effect of the inhibition of acidification in endosomes on DiI-signals. CNE1 cells expressing eGFP-Rab7 cultured in 35 mm glass-bottom culture dishes were pretreated with or without 20 mM NH_4Cl for 30 min at 37°C. DiI-exosomes were adsorbed to the cells for 30 min at room temperature in the presence or absence of NH_4Cl. Cells were then washed with the same medium and incubated for 5 h at 37°C in the presence or absence of NH_4Cl. Co-localization of DiI-exosomes (red) with eGFP-Rab7 (green) in the presence (right) or absence (left) of NH_4Cl was analyzed by using a confocal laser scanning microscope. Insets show DiI-exosomes (red), eGFP-Rab7 (green), and merged images of the boxed areas. The percentage of co-localization (proportion of co-localized DiI-exosomes with eGFP-fusion proteins to total DiI-exosomes) is shown in the individual panel. Scale bars: 20 μm.

Fig. 7. The effect of exosomes derived from Mutu cells on cell proliferation in the target cells.

CNE1 cells were grown in a 96-well plate in the absence or presence of DiI-exosomes (-) (white circle), exosomes (I) (gray circle), or exosomes (III) (black circle) for four days. As a control the cells were incubated with TNE buffer (black triangle). Cell proliferation was analyzed each

day. Each experiment was performed in triplicate and the results are presented as the mean ± SD. **, $P < 0.01$, *, $P < 0.05$ versus respective control (Student's *t* test).

Fig. 8. The effect of exosomes on ICAM-1 expression in the target cells.

(A) The effect of exosomes on ICAM-1 expression in CNE1 cells. CNE1 cells were grown in a 24-well plate in the absence or presence of DiI-exosomes (-), exosomes (I), or exosomes (III) for 24 h. ICAM-1 expression in CNE1 cells was measured by flow cytometry with an anti-ICAM-1 monoclonal antibody. Each experiment was performed in triplicate and the results are presented as the mean ± SD. *, $P < 0.05$ versus respective control (Student's *t* test). (B) Kinetics of ICAM-1 up-regulation in CNE1 cells. Shown is the expression of ICAM-1 at the indicated time points after a temperature shift following treatment with of DiI-exosomes (III). Each experiment was performed in triplicate and the results are presented as the mean ± SD. (C) ICAM-1 expression in CNE1 cells co-cultured with Mutu cells. CNE1 cells were co-cultured with Mutu$^-$, Mutu I, or Mutu III cells, which were grown on the membrane inserts, in the absence or presence of GM4869 for 72 h. ICAM-1 expression in CNE1 cells was measured by flow cytometry. Each experiment was performed in triplicate and the results are presented as the mean ± SD. *, $P < 0.05$ versus respective control (Student's *t* test).

Fig. 9. LMP1 was transferred to target cells *via* exosomes and contributed to the up-regulation of ICAM-1.

(A) LMP1 was transferred to CNE1 cells from Mutu III *via* exosomes. CNE1 cells were co-cultured with Mutu$^-$, Mutu I, or Mutu III cells, which were grown on the membrane inserts in the absence or presence of GM4869 for 72 h. LMP1 localization in CNE1 cells was analyzed by immunofluorescent staining. Nuclei were counterstained by DAPI. Scale bars: 20 μm. (B) Expression levels of LMP1 in Mutu cells. Mutu$^-$ that were transfected with a control or a LMP1 expression vector were harvested at 48 h post-transfection, and subjected to flow cytometric analysis along with Mutu III cells. Each experiment was performed in triplicate and the results are presented as the mean ± SD. (C) The effect of LMP1 expression on the up-regulation of ICAM-1 in CNE1 cells. CNE1 cells were co-cultured with Mutu$^-$ cells transfected with a control vector- or a LMP1 expression vector, which were grown in the membrane inserts in the absence or presence of GM4869 for 72 h. ICAM-1 expression in CNE1 cells was measured by flow cytometry. Each experiment was performed in triplicate and the results are presented as the mean ± SD. *, $P < 0.05$ versus respective control (Student's *t* test). (D) The effect of down-regulation of LMP1 on ICAM-1 expression in CNE1 cells.

CNE1 cells were co-cultured with control siRNA- or LMP1 siRNA-transfected Mutu III cells, which were grown in the membrane inserts for 72 h. ICAM-1 expression in CNE1 cells (white bars) and down-regulation of LMP1 (black bars) in Mutu III were measured by flow cytometry. Each experiment was performed in triplicate and the results are presented as the mean ± SD. *, $P < 0.05$ versus respective control (Student's *t* test).

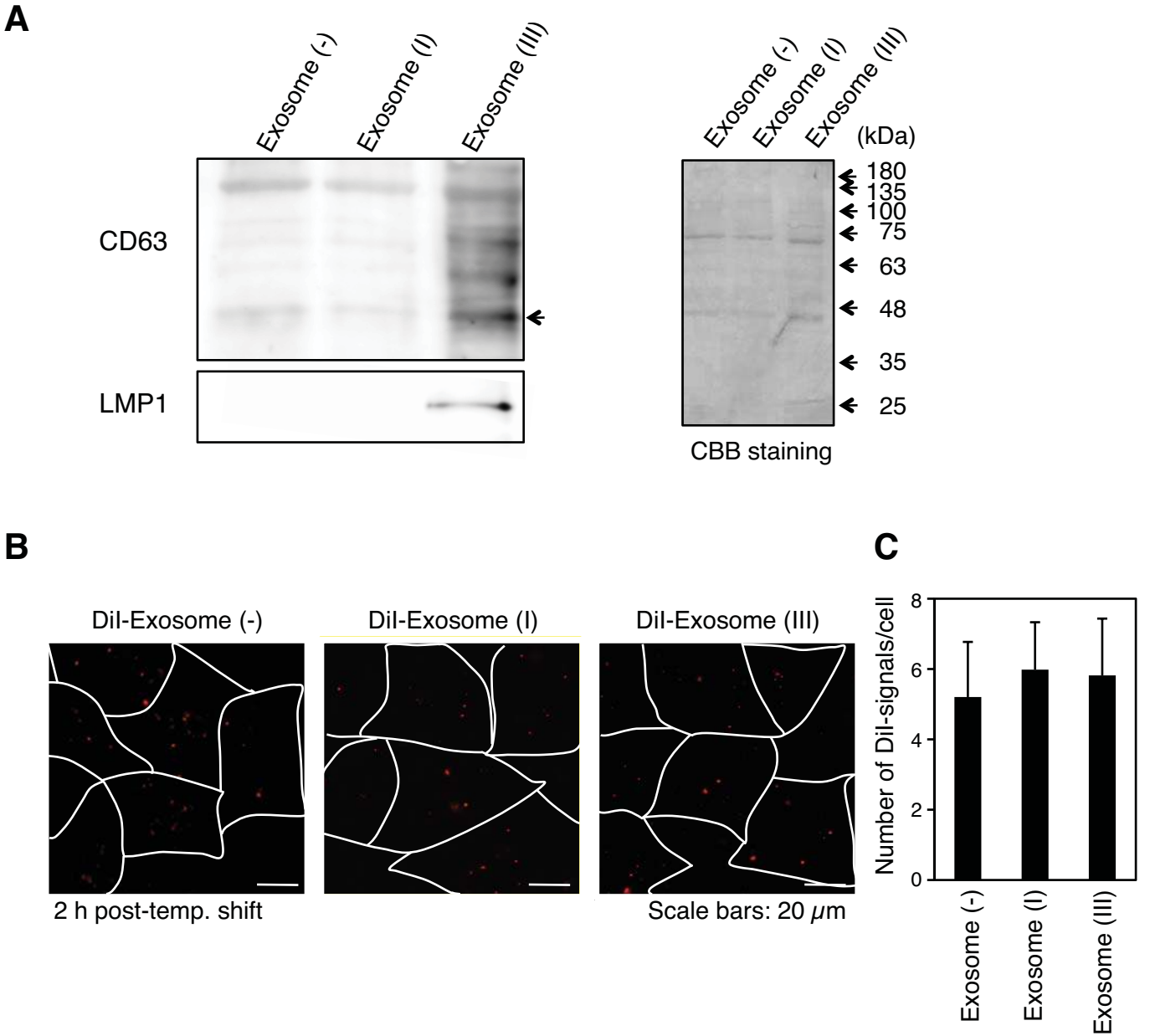
A
Exosome (-)
Exosome (I)
Exosome (III)
CD63
LMP1
Exosome (-)
Exosome (I)
Exosome (III)
(kDa)
180
135
100
75
63
48
35
25
CBB staining
B
DiI-Exosome (-)
DiI-Exosome (I)
DiI-Exosome (III)
2 h post-temp. shift
Scale bars: 20 μm
C
Number of DiI-signals/cell
0
2
4
6
8
Exosome (-)
Exosome (I)
Exosome (III)

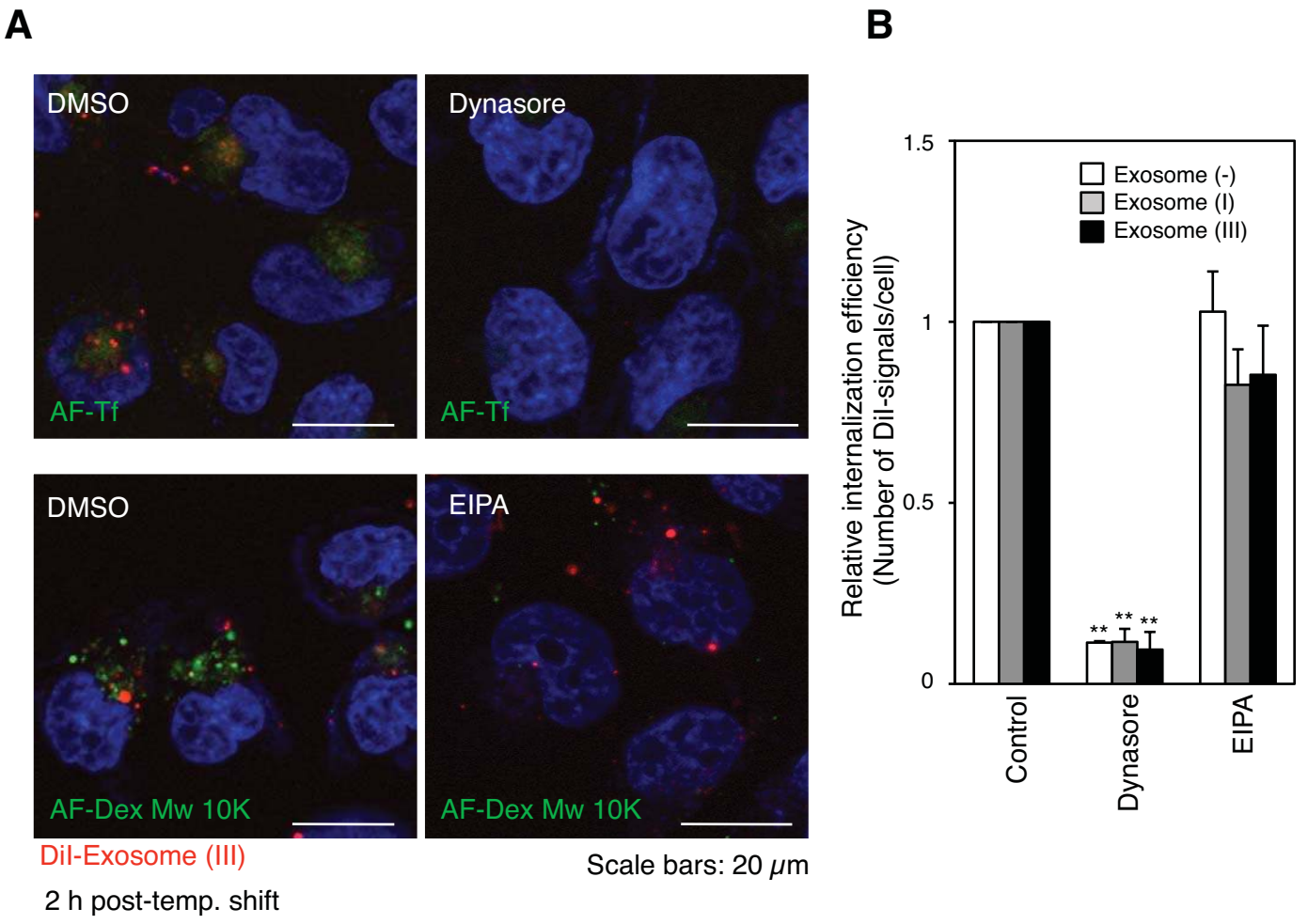
A
DMSO
AF-Tf
Dynasore
AF-Tf
DMSO
AF-Dex Mw 10K
EIPA
AF-Dex Mw 10K
DiI-Exosome (III)
2 h post-temp. shift
Scale bars: 20 μm
B
Relative internalization efficiency
(Number of DiI-signals/cell)
1.5
1
0.5
0
Exosome (-)
Exosome (I)
Exosome (III)
**
**
**
Control
Dynasore
EIPA

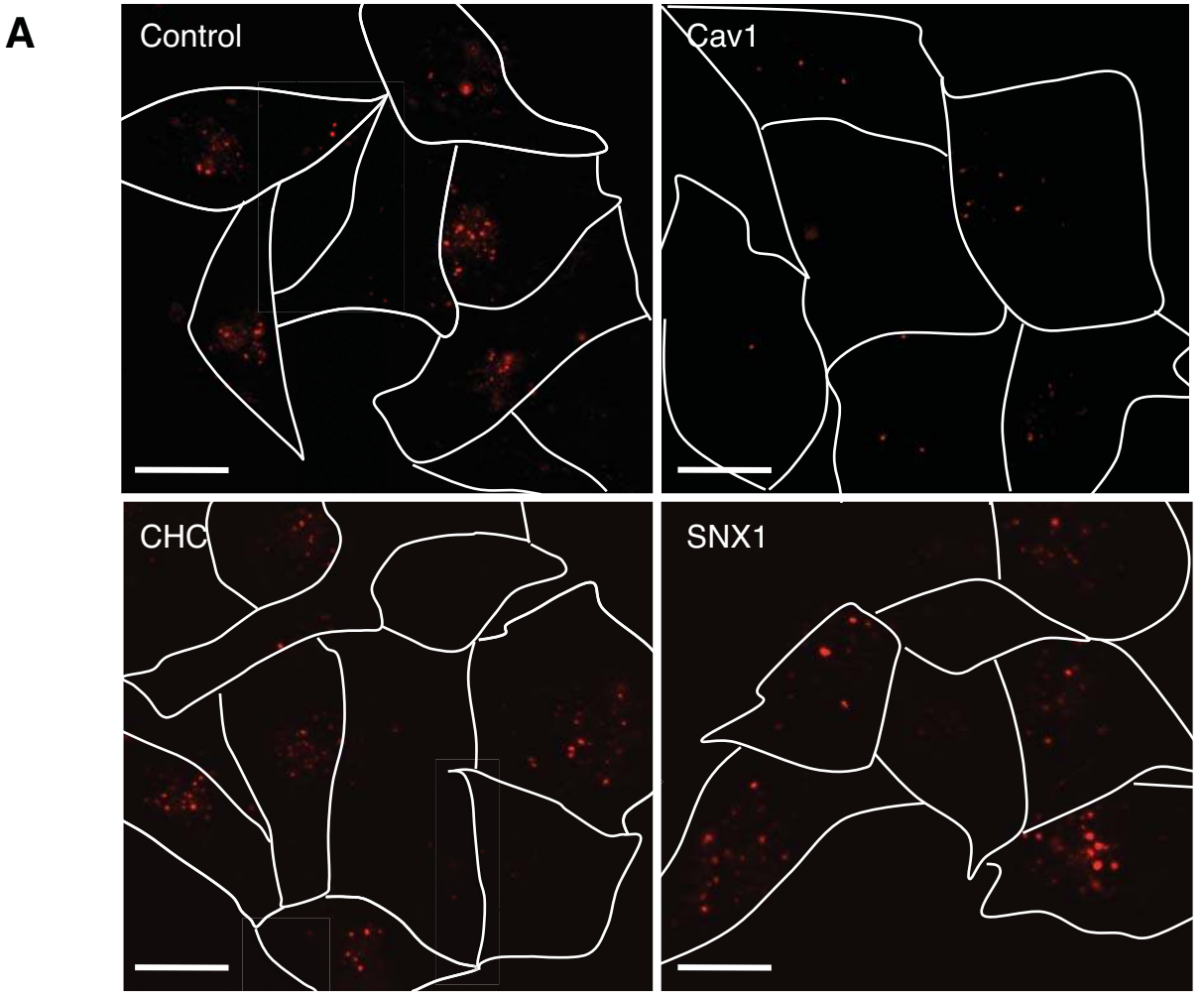
A
Control
Cav1
CHC
SNX1
2 h post-temp. shift
Scale bars: 20 μm

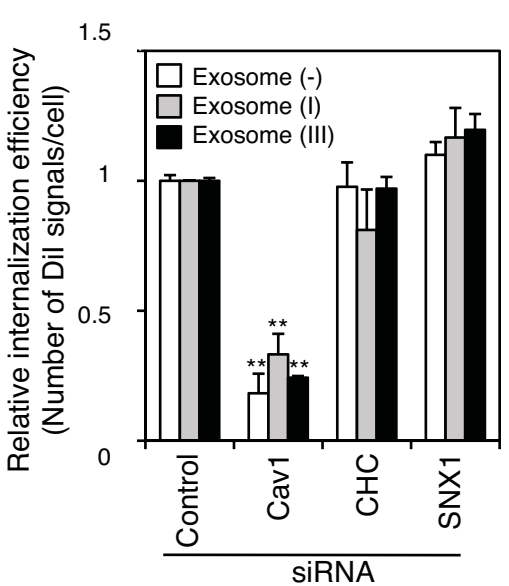
B
Relative internalization efficiency
(Number of DiI signals/cell)
1.5
1
0.5
0
Exosome (-)
Exosome (I)
Exosome (III)
**
**
**
Control
Cav1
CHC
SNX1
siRNA

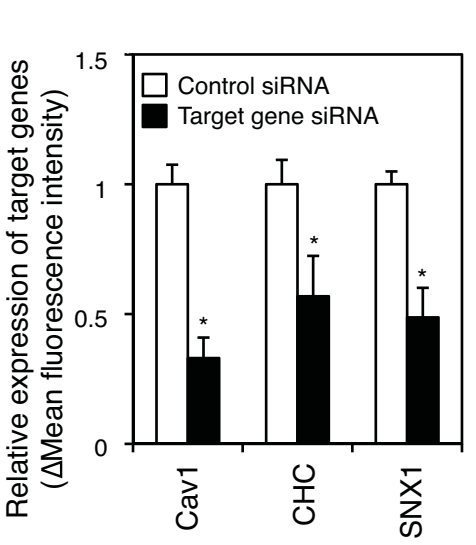
C
Relative expression of target genes
(ΔMean fluorescence intensity)
1.5
1
0.5
0
Control siRNA
Target gene siRNA
*
*
*
Cav1
CHC
SNX1

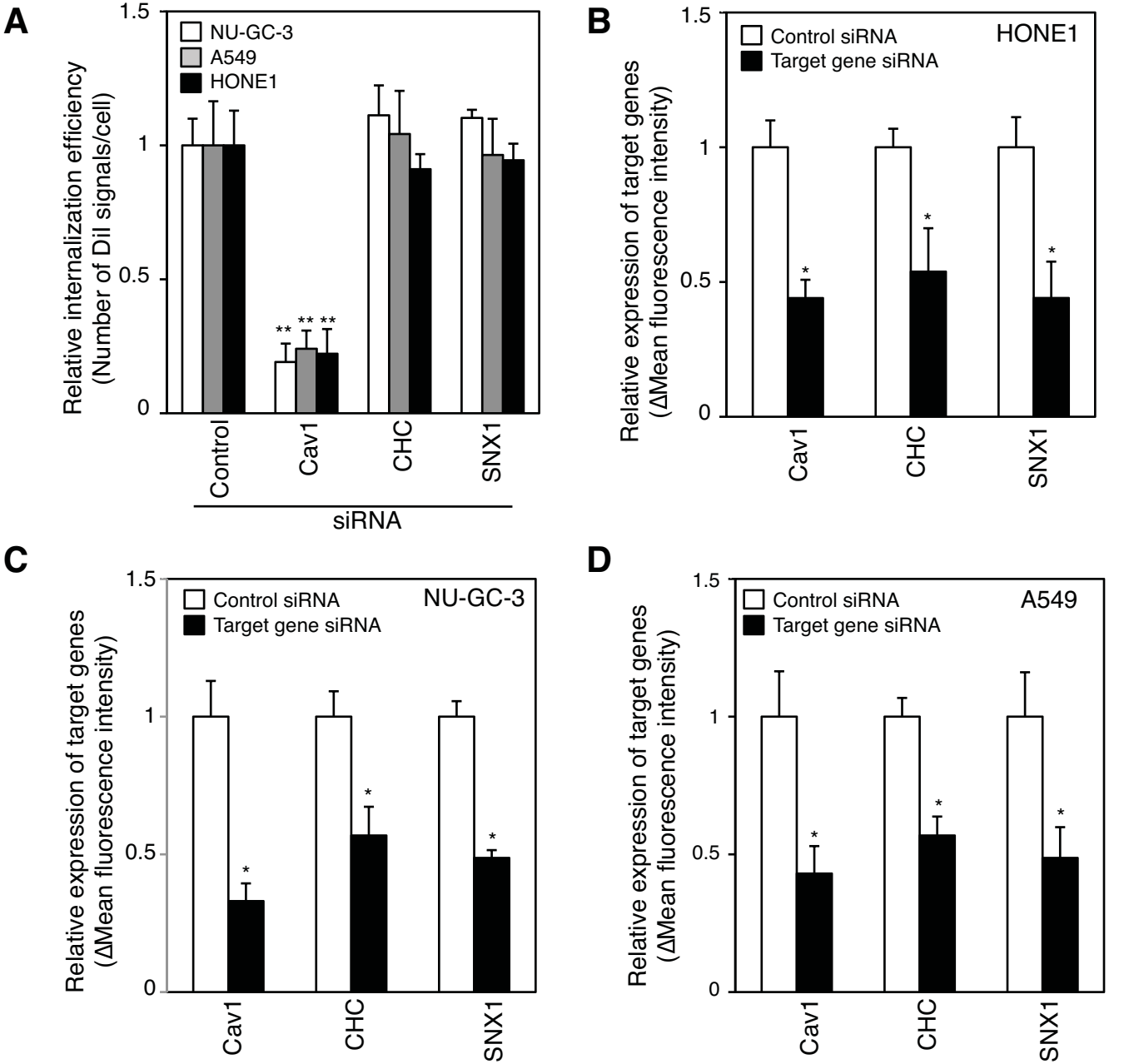
A
1.5
1
0.5
0
NU-GC-3
A549
HONE1
Relative internalization efficiency
(Number of DiI signals/cell)
**
**
**
Control
Cav1
CHC
SNX1
siRNA
B
Control siRNA
Target gene siRNA
HONE1
Relative expression of target genes
(ΔMean fluorescence intensity)
*
*
*
Cav1
CHC
SNX1
C
Control siRNA
Target gene siRNA
NU-GC-3
Relative expression of target genes
(ΔMean fluorescence intensity)
*
*
*
Cav1
CHC
SNX1
D
Control siRNA
Target gene siRNA
A549
Relative expression of target genes
(ΔMean fluorescence intensity)
*
*
*
Cav1
CHC
SNX1

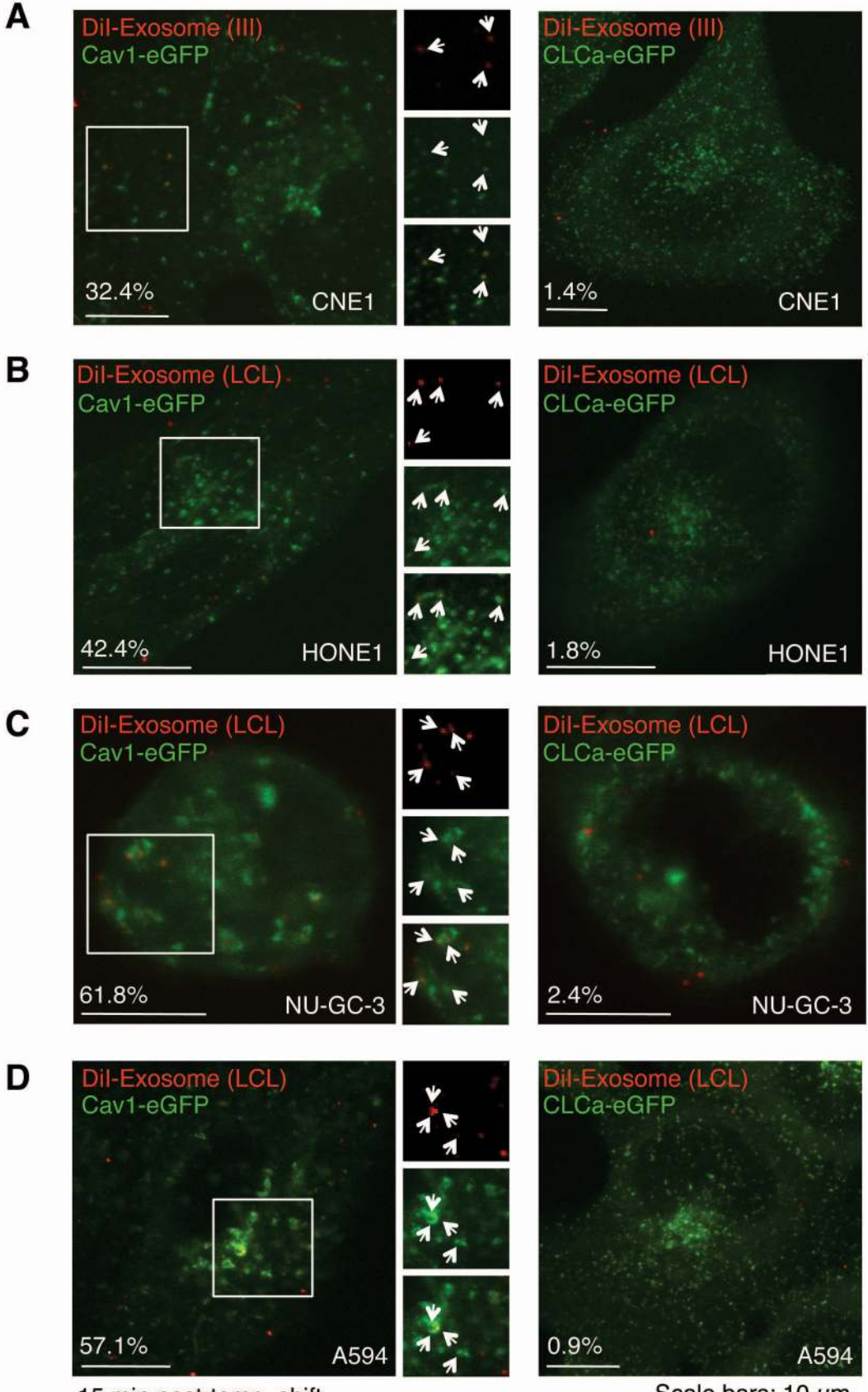
A
DiI-Exosome (III)
Cav1-eGFP
32.4%
CNE1
DiI-Exosome (III)
CLCa-eGFP
1.4%
CNE1
B
DiI-Exosome (LCL)
Cav1-eGFP
42.4%
HONE1
DiI-Exosome (LCL)
CLCa-eGFP
1.8%
HONE1
C
DiI-Exosome (LCL)
Cav1-eGFP
61.8%
NU-GC-3
DiI-Exosome (LCL)
CLCa-eGFP
2.4%
NU-GC-3
D
DiI-Exosome (LCL)
Cav1-eGFP
57.1%
A594
DiI-Exosome (LCL)
CLCa-eGFP
0.9%
A594
15 min post-temp. shift
Scale bars: 10 μm

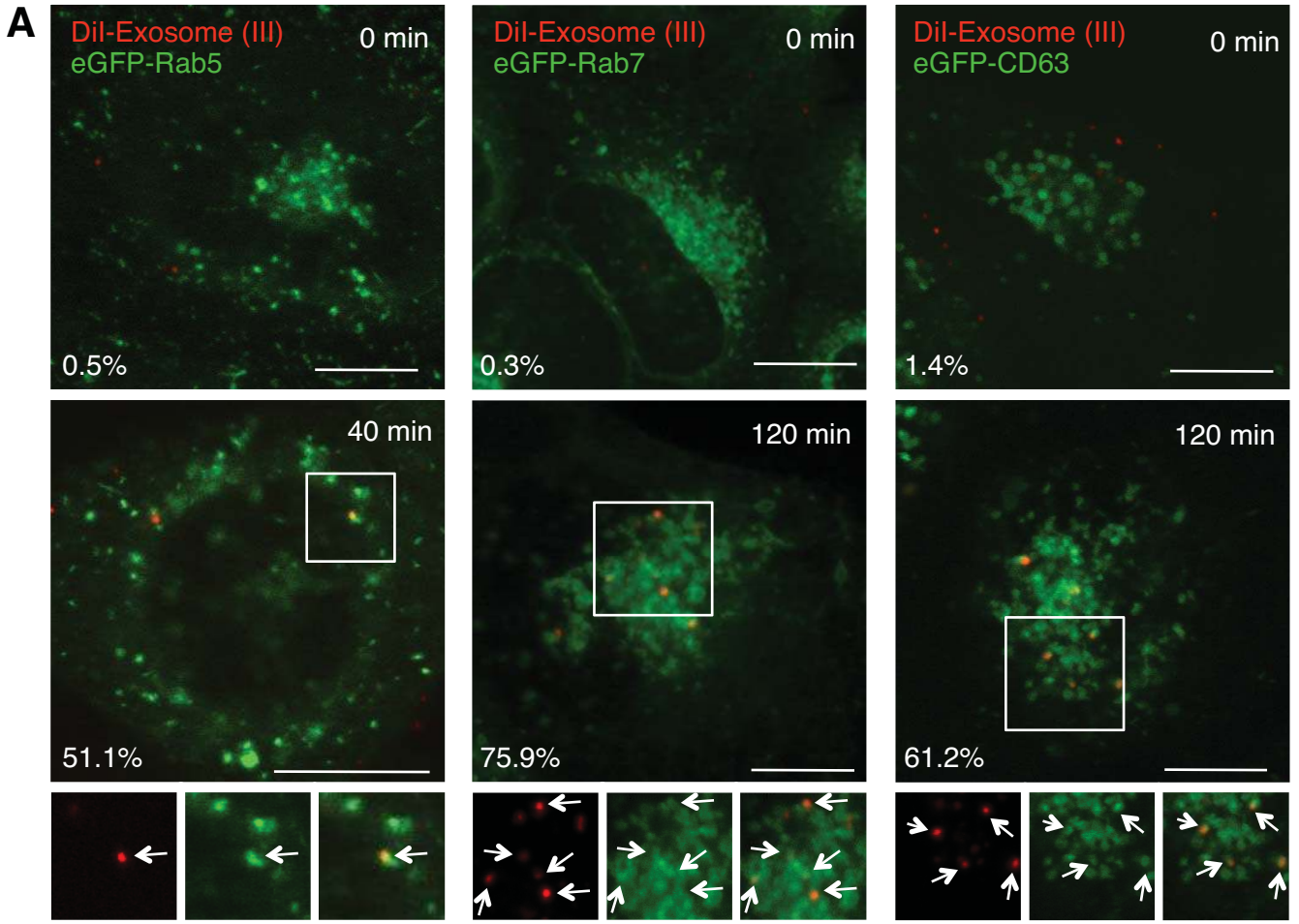
A
DiI-Exosome (III)
eGFP-Rab5
0 min
0.5%
DiI-Exosome (III)
eGFP-Rab7
0 min
0.3%
DiI-Exosome (III)
eGFP-CD63
0 min
1.4%
40 min
51.1%
120 min
75.9%
120 min
61.2%
Scale bars: 20 μm
B
% of co-localization of DiI-exosomes with Rab5
Exosome (-)
Exosome (I)
Exosome (III)
0
10
20
30
40
50
60
120
C
% of co-localization of DiI-exosomes with Rab7
Exosome (-)
Exosome (I)
Exosome (III)
0
30
60
90
150
Time (min)
D
Control
DiI-Exosome (III)
eGFP-Rab7
73.2%
NH4Cl
DiI-Exosome (III)
eGFP-Rab7
65.8%
5 h post-temp. shift
Scale bars: 20 μm

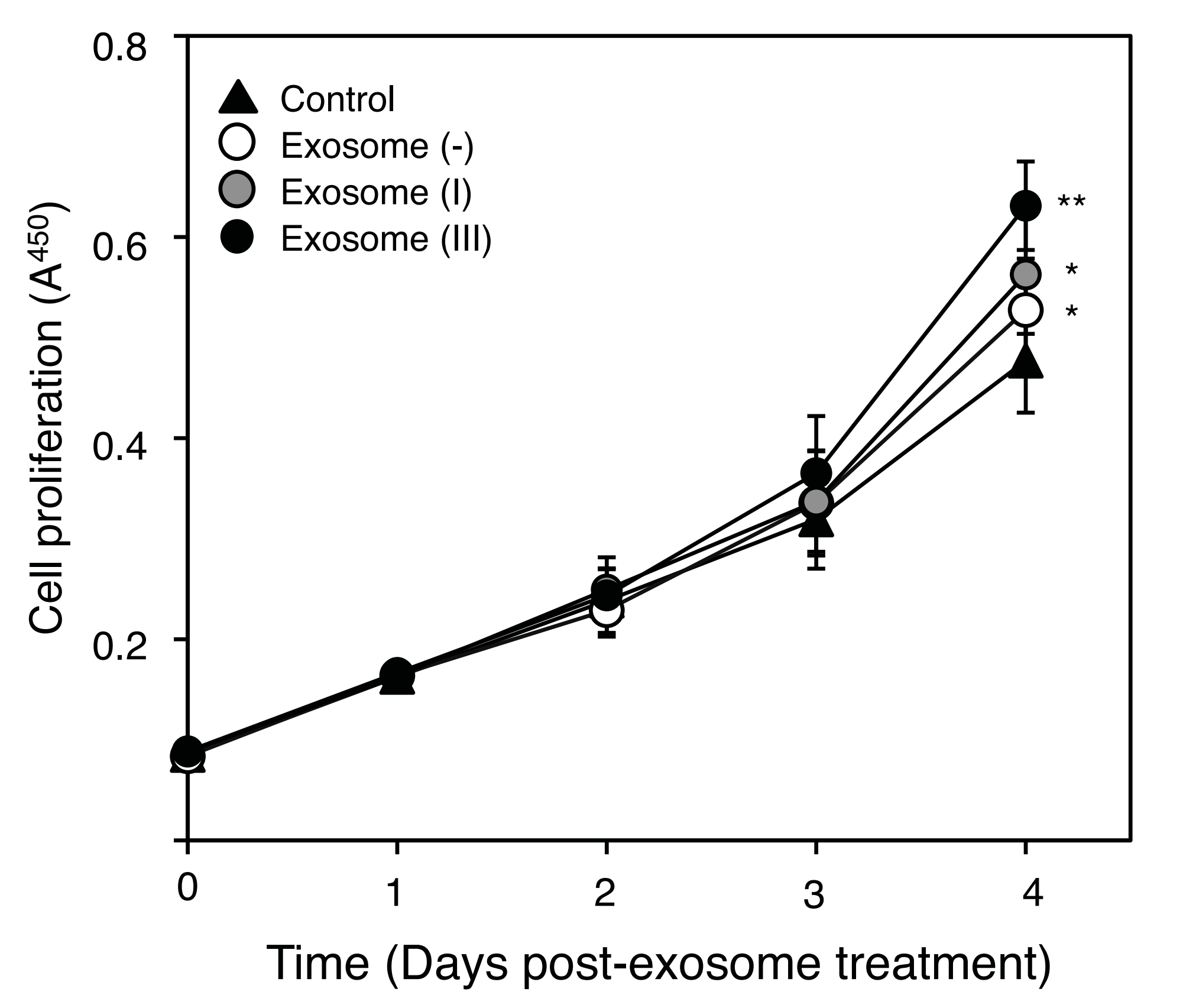
Control
Exosome (-)
Exosome (I)
Exosome (III)
**
*
*
0.8
0.6
0.4
0.2
0
1
2
3
4
Cell proliferation (A450)
Time (Days post-exosome treatment)

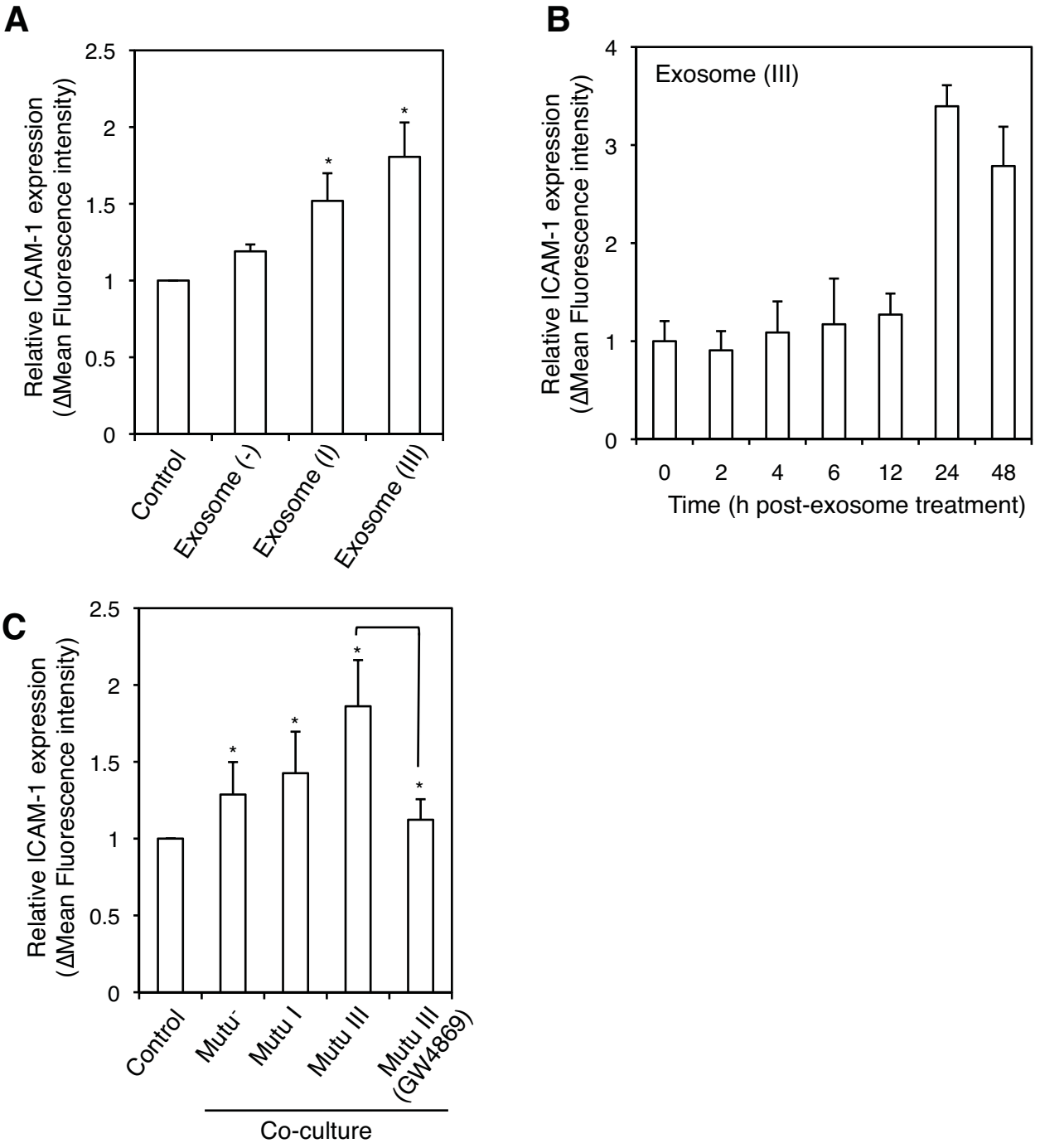
A
Relative ICAM-1 expression
(ΔMean Fluorescence intensity)
2.5
2
1.5
1
0.5
0
*
*
Control
Exosome (-)
Exosome (I)
Exosome (III)
B
Relative ICAM-1 expression
(ΔMean Fluorescence intensity)
Exosome (III)
4
3
2
1
0
0
2
4
6
12
24
48
Time (h post-exosome treatment)
C
Relative ICAM-1 expression
(ΔMean Fluorescence intensity)
2.5
2
1.5
1
0.5
0
*
*
*
*
Control
Mutu-
Mutu I
Mutu III
Mutu III
(GW4869)
Co-culture

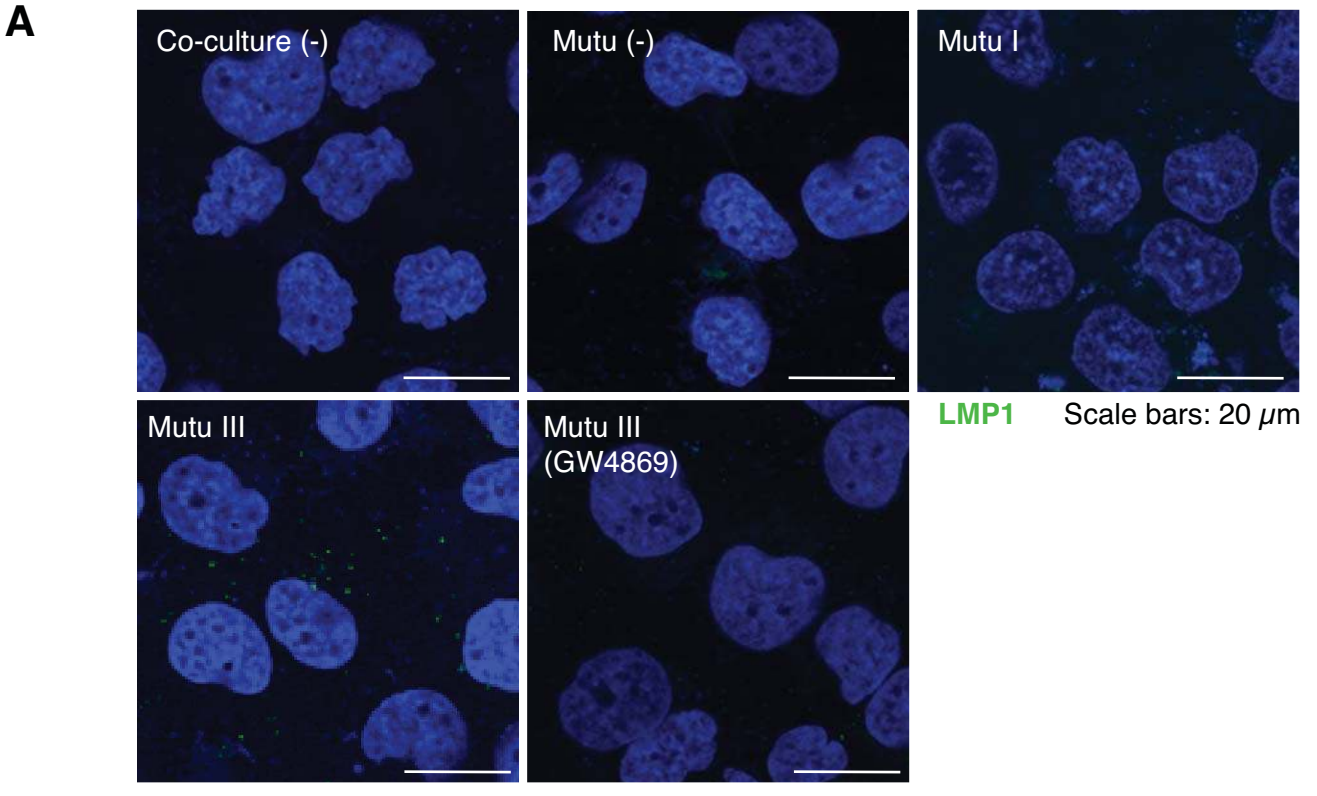
A
Co-culture (-)
Mutu (-)
Mutu I
Mutu III
Mutu III
(GW4869)
LMP1
Scale bars: 20 μm

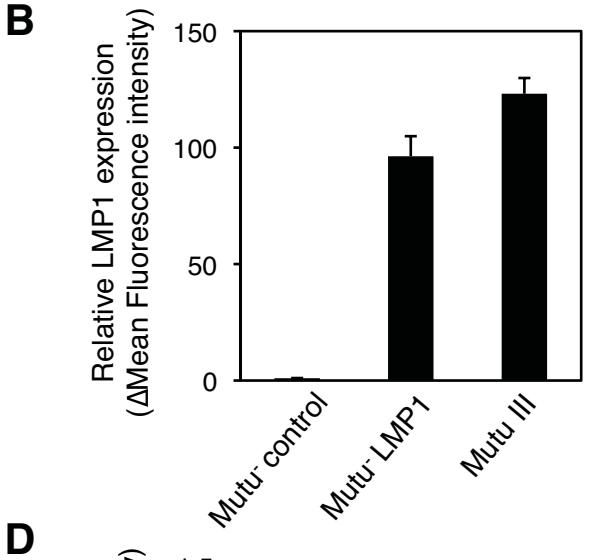
B
Relative LMP1 expression
(ΔMean Fluorescence intensity)
150
100
50
0
Mutu⁻control
Mutu⁻LMP1
Mutu III

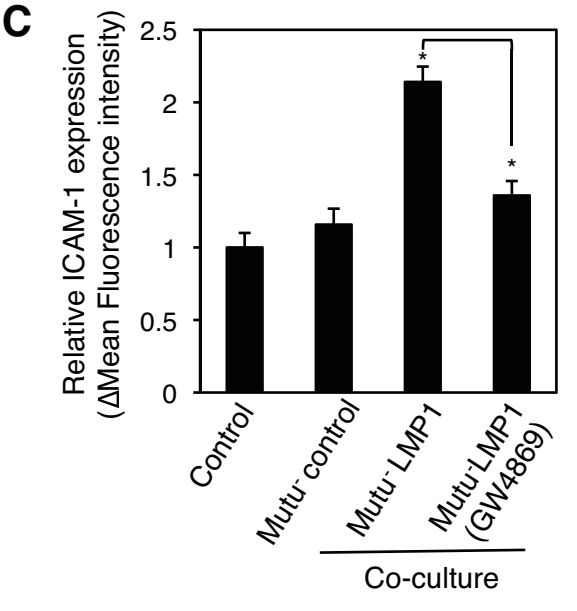
C
Relative ICAM-1 expression
(ΔMean Fluorescence intensity)
2.5
2
1.5
1
0.5
0
*
*
Control
Mutu⁻control
Mutu⁻LMP1
Mutu⁻LMP1
(GW4869)
Co-culture

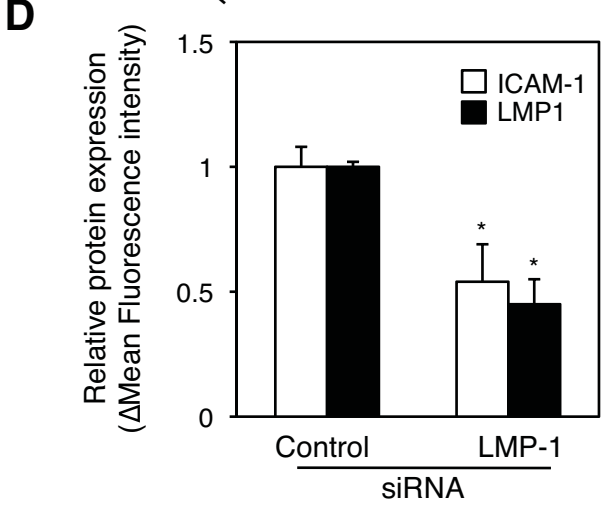
D
Relative protein expression
(ΔMean Fluorescence intensity)
1.5
1
0.5
0
ICAM-1
LMP1
*
*
Control
LMP-1
siRNA